EAI Endorsed Transactions
on Mobile Communications and Applications

5G NR Uplink Performance Optimization: A Comprehensive Study on PRACH and PUSCH Interference Management

Désiré Guel[1], P. Justin Kouraogo[1], Flavien Hervé Somda[1], Boureima Zerbo[2], Oumarou Sié[3]

[1]Université Joseph KI-ZERBO (U-JKZ), Burkina Faso
[2]Université Thomas SANKARA (UTS), Burkina Faso
[3]Université Aube Nouvelle, Ouagadougou, Burkina Faso

Abstract

The evolution of 5G New Radio (NR) technology offers unprecedented speeds, ultra-low latency, and the capability to connect billions of devices. However, these advancements come with significant challenges, particularly in managing interference during uplink communication. This study presents a comprehensive investigation into the optimization of 5G NR uplink performance by focusing on two critical channels: the Physical Uplink Shared Channel (PUSCH) and the Physical Random Access Channel (PRACH). The research explores the impact of intra-cell and inter-cell interference on these channels, highlighting how various User Equipment (UE) and cell configuration parameters influence performance. Key Performance Indicators (KPIs) such as Block Error Rate (BLER) and Correct Detection Rate (CDR) are utilized to assess the effectiveness of proposed interference management strategies. Through rigorous simulations and empirical evaluations, the study provides valuable insights into optimizing 5G NR networks, aiming to enhance the robustness and reliability of uplink communication in diverse interference scenarios. The findings underscore the importance of adaptive resource allocation and interference mitigation techniques in achieving superior network performance and quality of service (QoS).

Received on 24 August 2024; accepted on 22 March 2025; published on 08 April 2025

Keywords: 5G-NR , Physical Random Access Channel (PRACH), PUSCH, Intra/Inter-Cell Interference, Quality of Service (QoS), Block Error Rate (BLER)

doi:10.4108/eetmca.6933

1. Introduction

The advent of 5G NR (New Radio) technology has unlocked a new realm of possibilities in wireless communication, promising unprecedented speeds, ultra-low latency, and the capacity to connect billions of devices simultaneously [1–5]. However, the robustness and reliability of 5G NR networks in real-world scenarios depend heavily on the ability to effectively manage and mitigate interference, both within cells (intra-cell interference) and between neighboring cells (inter-cell interference) [6–8].

Despite significant advancements in interference management, existing approaches often fall short in addressing the dynamic nature of interference in ultra-dense networks. Current methodologies rely heavily on predefined scheduling mechanisms and static interference mitigation techniques, which struggle to adapt to rapidly changing interference patterns [9, 10]. This study bridges this gap by proposing a novel framework that integrates adaptive resource allocation and interference-aware detection mechanisms tailored for 5G NR uplink channels.

In the pursuit of seamless connectivity and enhanced user experiences, the performance of key uplink channels, namely the Physical Uplink Shared Channel (PUSCH) and the Physical Random Access Channel

*Corresponding author. Email: desire.guel@ujkz.bf

(PRACH), plays a critical role. The 5G-NR PUSCH serves as the primary uplink communication channel for User Equipment (UE) to transmit data to the network, while the PRACH acts as the gateway for UE to initiate communication with the network [11–13]. The efficiency of both channels is profoundly influenced by surrounding interference conditions, making them essential components of the 5G NR architecture [9, 10].

Intra-cell interference arises when multiple UEs within the same cell transmit data or attempt to access the network simultaneously, leading to contention for PUSCH and PRACH resources [14, 15]. Conversely, inter-cell interference emerges when UEs from neighboring cells contend for the same resources, leading to contention across cell boundaries [16, 17]. These interference scenarios introduce complexities in both PUSCH and PRACH detection, impacting network efficiency, latency, and overall Quality of Service (QoS) [18, 19].

This article embarks on a comprehensive study to address these challenges by introducing an interference-aware framework for optimizing 5G-NR PUSCH and PRACH performance. Unlike conventional interference mitigation strategies, our approach dynamically adapts to network conditions, leveraging machine learning-driven resource allocation and signal processing enhancements to improve detection reliability. By systematically analyzing the impact of UE and cell configurations on PUSCH and PRACH performance, we identify key bottlenecks and propose novel interference mitigation strategies [20].

Our investigation explores a spectrum of aspects, including resource allocation strategies and adaptive interference mitigation techniques. Through rigorous simulations and empirical evaluations, we demonstrate how these novel methodologies significantly enhance the resilience of PUSCH and PRACH against both intra-cell and inter-cell interference. Our findings provide valuable insights into optimizing uplink transmission in dense 5G networks, contributing to improved spectral efficiency and reduced access latency [21].

The remainder of this article is organized as follows: Section 2 reviews the fundamental principles and intricate processes underlying the 5G New Radio (NR) Random Access (RA) and PUSCH transmission. Next, Section 3 discusses related work on interference management in 5G NR networks, highlighting the limitations of existing approaches. Following that, Section 4 outlines the proposed methodology, providing details on the simulation setup and key parameters considered. Then, Section 5 presents a comparative analysis of PUSCH and PRACH performance under various interference conditions, thereby demonstrating the effectiveness of our proposed strategies. Finally, Section 6 concludes the article by summarizing our key contributions and suggesting potential directions for future research.

2. NR Random Access and PUSCH Transmission: Principles and Processing

This section reviews the fundamental principles and intricate processes underlying the 5G New Radio (NR) Random Access (RA) and PUSCH transmission.

2.1. PRACH Principle and Preamble Detection

This section presents the essential aspects of Random Access (RA) in 5G-NR context. Preambles play a crucial role in synchronization, initial access, and signal detection.

Preamble Structure and Procedure. Random access (RA) is a basic procedure in 5G-NR technologies, enabling UEs to establish uplink synchronization and initiate uplink transmission. PRACH employs phase modulation based on Zadoff-Chu sequences [22] with distinct phase variations among different symbols within the sequences. Before sending its random access request, UEs must retrieve a set of information transmitted by the base station through the SIB2 *(System Information Block Type 2)* message [**TS138331**].

With this information, the UE can transmit the PRACH preamble using the resources indicated by the Next-Generation NodeB (gNB) during the transmission of SIB2. The transmission of the PRACH is associated with the RA-RNTI *(Random Access RNTI)*.

When an UE enters a new cell, it has no prior knowledge of the gNB. After identifying the optimal SSB *(Synchronization Signal Block)* through downlink synchronization, the UE transmits the PRACH containing its information, based on the best time index of the SSB. Figure 1 illustrates the interactions between the UE and the gNB during the initial access procedure [5].

Random access process is described in Figure 1. The UE selects randomly a preamble from a list of parameters broadcasted through the SIB2 and transmits it in the PRACH with an initial power result of a basic downlink pathloss estimation. If there is no answer from the gNB, the UE makes a retry with higher power level.

The 5G-NR PRACH preamble consisted of a complex sequence (SEQ) which an OFDM symbol, built with a Cyclic Prefix (CP), thus allowing for an efficient frequency-domain receiver at the gNB. The preamble length is shorter than the PRACH slot in order to provide room for a Guard Period (GP) to absorb the propagation delay. The CP facilitates PRACH processing in the frequency domain. Refer to Figure 2 for the NR-PRACH structure.

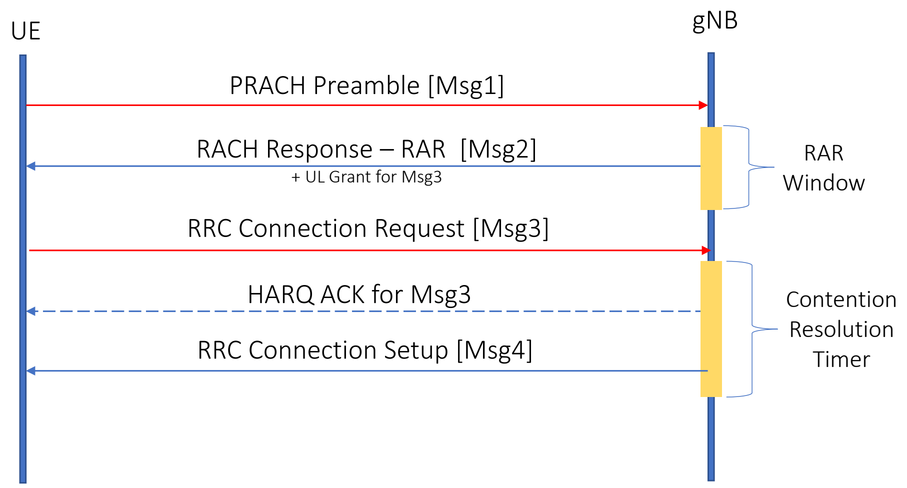

Figure 1. NR-PRACH Procedure.

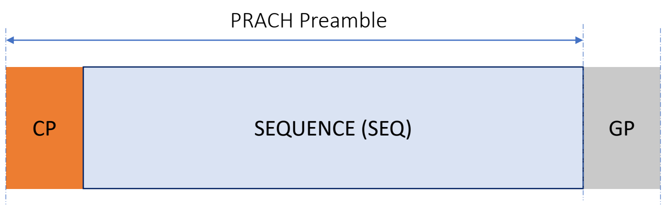

Figure 2. NR-PRACH structure.

Preamble Sequence Generation. The preamble sequence length is set to a prime number of 839, there are 838 sequences with optimal cross?correlation properties. The u^{th} $(0 \leq u \leq 837)$ root Zadoff-Chu sequence is defined by (Nzc is the length of the Zadoff-Chu sequence):

$$x_u(n) = e^{-j\frac{\pi u n(n+1)}{N_{ZC}}}, 0 \leq n \leq N_{ZC} - 1 \qquad (1)$$

From the u^{th}root ZC sequence, random access preambles with Zero Correlation Zones *(ZCZ)* of length $N_{ZC} - 1$ are defined by Cyclic Shifts *(CS)* according to [**3GPPTS36211V890**]:

$$x_{u,v}(n) = x_u((n + C_v) \bmod N_{ZC}), \qquad (2)$$

where C_v is the cyclic shift, and N_{ZC} is the cyclic shift offset. This paper adopts preamble format 0 in the 5G-NR, which generates from a 839 point ZC sequence which is specifically designed for contention-based access, where multiple UEs may attempt to access the network simultaneously.

Preamble Detection . The PRACH receiver is implemented to maximize the probability of "correct" preamble detection and minimize processing latency. The functional diagram of the conventional PRACH receiver which shares certain operations with the Orthogonal Frequency Division Multiplexing (OFDM) demodulator is illustrated in Figure 3. The 5G-NR PRACH receiver process [23] :

(1) *CP-GP (Cyclic Prefix and Guard Period) Removal*: In this step, the Cyclic Prefix (CP) and Guard Period (GP), which are added to the transmitted PRACH signal for synchronization purposes, are removed to obtain the original signal.

(2) *Frequency Shift*: The received signal is shifted in frequency to bring it to a common reference frequency, aligning it with the system's reference.

(3) *Decimation*: The signal is sampled at a lower rate, reducing the data rate while retaining essential information, to simplify subsequent processing.

(4) *FFT (Fast Fourier Transform)*: An FFT is applied to the decimated signal to transform it from the time domain to the frequency domain, allowing the identification of frequency components.

(5) *Sub-Carrier Demapping*: In this step, sub-carriers used for the PRACH signal are demapped, extracting the relevant information from the frequency domain representation.

(6) *IFFT (Inverse Fast Fourier Transform)*: An IFFT is performed to convert the signal back from the frequency domain to the time domain, preparing it for further processing.

(7) *Signature Detection*: Finally, signature detection technique is applied to identify and extract specific patterns or signatures in the PRACH signal, which are crucial for synchronization and channel estimation in 5G-NR communication systems. Figure 4 shows the basic functions of the signature detector.

The fact that different PRACH signatures are generated from Cyclic Shifts *(CS)* of a common root sequence means that the frequency-domain computation of the Power Delay Profile *(PDP)* of a root sequence provides in one shot the concatenated PDPs of all signatures derived from the same root sequence. Therefore, the signature detection process consists of searching, within each ZCZ defined by each Cyclic Shifts (CS), the PDP peaks above a detection threshold over a search window corresponding to the cell size.

(1) *Power Correlation Extraction*: In this step, the received signal's power is correlated with a known "root sequence" to identify potential preamble candidates within the received signal. This process helps in locating the start of the frame.

(2) *Detection threshold Calculation*. The target false alarm probability $p_{fa}(T_{\text{det}})$ drives the setting of the detection threshold T_{det}. In [23], it is showed that under the assumption that the L samples in the uncertainty window are uncorrelated Gaussian noise with variance σ_n^2 in the absence of preamble transmission, the complex sample sequence $z_a^m(\tau)$ received from antenna a (delayed to reflect a targeted time offset τ of the search window, and despread over a coherent accumulation length (in samples) N_{ca} against the reference code sequence) is a complex Gaussian random variable with variance $\sigma_{n,ca}^2 = N_{ca} \times \sigma_n^2$. In practice, N_{ca} is the size of the IFFT. The non-coherent accumulation $z_{nca}(\tau)$ is modelled as follows [23] :

$$z_{nca}(\tau) = \sum_{a=1}^{N_a} \sum_{m=0}^{N_{nca}-1} |z_a^m(\tau)|^2 \tag{3}$$

where N_a is the number of antennas and N_{nca} is the number of additional non-coherent accumulations (e.g. in case of sequence repetition).

$z_{nca}(\tau)$ follows a central chi-square distribution with $2N = 2N_a \times N_{nca}$ degrees of freedom, with mean (defining the noise floor) $\gamma_n = N \times \sigma_{n,ca}^2$ and Cumulative Distribution Function (CDF) $F(T_{\text{det}}) = 1 - p_{fa}(T_{\text{det}})^L$. It is worth noticing that instead of the absolute threshold , in [23] the authors consider the threshold T_r relative to the noise floor γ_n as follows:

$$T_r = \frac{T_{\text{det}}}{\gamma_n} = \frac{T_{\text{det}}}{N_a \times N_{nca} N_{ca} \sigma_n^2} \tag{4}$$

(3) *Correlation Window Extraction:* The received signal is divided into smaller time intervals or windows to focus the correlation process on specific parts of the signal. These windows allow for more precise identification of the preamble within the signal.

(4) *Peak Search:* Within each correlation window, the highest correlation peak is identified. This peak corresponds to the position where the preamble sequence aligns most closely with the received signal, indicating the start of the frame.

(5) *Timing Advance (TA) Calculation:* Once the peak is found, the timing advance (TA) is calculated to determine the timing misalignment between the received signal and the expected frame timing. The TA is used to synchronize the receiver with the incoming signal for further data reception and processing.

2.2. PUSCH Transmission and Reception

The Physical Uplink Shared Channel (PUSCH) is used for data transmission from the User Equipment (UE) to the base station. This subsection provides a detailed overview of the transmission and reception process of PUSCH. Figure 5 illustrates the entire process from the transmission of the NR-PUSCH to its reception and decoding. It is including the critical stages involved in handling intra-cell and inter-cell interference. The 5G-NR PUSCH transmission and reception process:

(1) *UL-SCH (Uplink Shared Channel) Encoding*: The process begins with the encoding of the data to be transmitted on the Uplink Shared Channel (UL-SCH). This step involves adding error correction codes and other necessary information to the data, ensuring robust communication over the wireless channel.

(2) *PUSCH Modulation*: The encoded UL-SCH data is then modulated onto the Physical Uplink Shared Channel (PUSCH). Modulation maps the encoded data onto the specific frequency and time resources allocated for the uplink transmission in the 5G-NR system.

(3) *Implementation-Specific Precoding*: Before transmission, the modulated signal undergoes implementation-specific precoding. Precoding prepares the signal for transmission by optimizing it according to the specific antenna configuration and channel conditions, improving the signal's robustness against interference and channel impairments.

(4) *CP-OFDM (Cyclic Prefix-Orthogonal Frequency Division Multiplexing)*: The pre-coded signal is

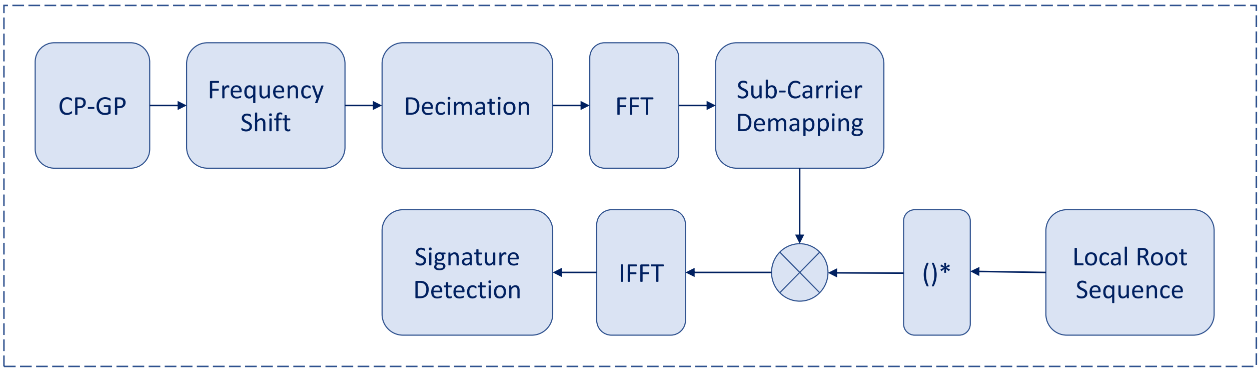

Figure 3. 5G-NR PRACH Receiver Block Diagram.

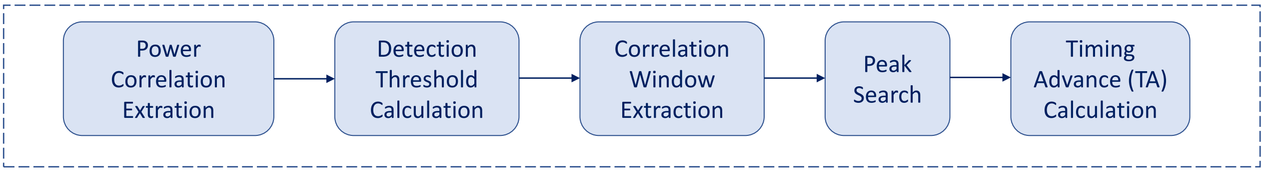

Figure 4. Preamble Detection Block Diagram

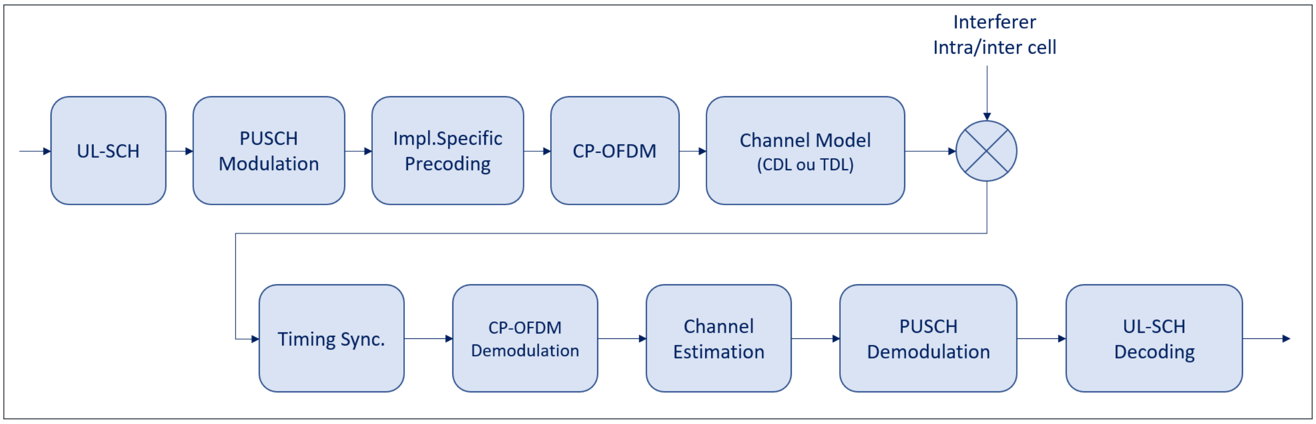

Figure 5. Transmission and Reception of the NR-PUSCH.

then processed through CP-OFDM. This step adds a Cyclic Prefix (CP) to the OFDM symbols, which helps mitigate inter-symbol interference and maintains orthogonality between subcarriers during transmission.

(5) *Channel Model (CDL or TDL)*: The signal is transmitted through a channel modeled using either a Clustered Delay Line (CDL) or Tapped Delay Line (TDL) approach. These models simulate the real-world propagation conditions that the signal will encounter, including the effects of multipath, Doppler shift, and fading. Additionally, the diagram accounts for intra-cell and inter-cell interference that may affect the received signal.

(6) *Timing Synchronization*: Upon reception, the first step is timing synchronization which aligns the received signal in time with the receiver's internal clock. This is important for accurately demodulating the signal and ensuring that it is correctly aligned with the expected frame structure.

(7) *CP-OFDM Demodulation*: The synchronized signal is then demodulated using CP-OFDM. This step involves removing the Cyclic Prefix and converting the signal back into the frequency domain to recover the individual subcarrier components.

(8) *Channel Estimation*: After demodulation, channel estimation is performed. The receiver estimates

the characteristics of the channel through which the signal has propagated by using reference signals embedded in the received data. This estimation is essential for accurately decoding the data and mitigating the effects of the channel.

(9) *PUSCH Demodulation*: After the channel is estimated, the receiver proceeds to demodulate the PUSCH. This step recovers the original data bits from the modulated signal by using the channel estimates to compensate any distortions introduced by the channel.

(10) *UL-SCH Decoding*: The demodulated data is decoded to retrieve the original information sent on the UL-SCH. Error correction codes are applied to correct any errors that may have occurred during transmission, ensuring the integrity of the received data.

3. Related Works

This section explores various studies related on PRACH and PUSCH interference management. The Table 1 presents the related works categorized into relevant sections such as Channel Estimation, Deep Learning, Interference Management and Full-Duplex Systems. This categorization helps in understanding the scope of research covered and the contributions of each reference in the context of PRACH and PUSCH interference management.

3.1. Channel Estimation

Channel estimation plays a crucial role in wireless communication, particularly in 5G-NR, where it directly impacts signal recovery and system performance. Traditional methods, such as Least Squares (LS) and Minimum Mean Squared Error (MMSE), offer limited accuracy in dynamic environments. Recent advancements leverage deep learning and machine learning to enhance estimation accuracy and robustness against noise and interference.

Several studies have explored novel channel estimation techniques for 5G-NR systems. Song et al. [20] proposed a Double-Threshold (DT) method based on Adaptive Frame Statistics (AFS), improving accuracy by distinguishing between noise and multipath components. Gu et al. [16] introduced a Manifold Learning and Extreme Learning Machine (ML-ELM)-based method, specifically tailored for mmWave Massive MIMO, addressing high-dimensional channel estimation challenges. Table 2 provides a comparative analysis of various channel estimation techniques, highlighting their key benefits, weaknesses, and relevant references from the literature.

Comparison with Prior Research. Compared to conventional methods, recent approaches utilizing deep learning significantly outperform LS and MMSE in high-noise environments. Haq et al. [19] demonstrated that Deep Neural Networks (DNNs) adapt dynamically to changing channel conditions, improving real-time performance. However, the computational complexity of deep learning-based methods remains a barrier to real-time applications, as noted by Li et al. [17].

Machine Learning-Based Interference Mitigation. Advanced learning techniques, including Convolutional Neural Networks (CNNs) and Generative Adversarial Networks (GANs), have been applied to refine channel estimation. Doshi et al. [9] showed that GANs, trained over-the-air (OTA), enhance estimation accuracy in mmWave MIMO, mitigating interference more effectively than conventional models.

3.2. Deep Learning in 5G-NR

Deep learning (DL) has revolutionized physical layer processing in 5G-NR, with applications ranging from channel estimation to interference management. DL models leverage large datasets to learn complex signal patterns, making them well-suited for highly dynamic network environments.

Ozpoyraz et al. [6] provided an extensive survey of DL applications in 5G, highlighting their impact on massive MIMO and multi-carrier systems. Boas et al. [7] further explored AI-driven channel estimation, emphasizing adaptability and efficiency.

Comparison with Prior Research. While traditional techniques rely on predefined models, DL-based methods can adapt to unseen channel conditions. Shammaa et al. [8] demonstrated that adaptive deep learning receivers outperform conventional systems in full-duplex environments, dynamically adjusting to interference.

Interference Mitigation using AI. AI-driven models, such as reinforcement learning-based interference alignment [27], have shown promise in mitigating interference in dense networks. However, high computational complexity and the requirement for large labeled datasets remain significant challenges [9].

3.3. Interference Management

Efficient interference management is crucial in 5G-NR networks to ensure seamless communication. Techniques such as interference alignment [11], topological interference management [26], and machine learning-based approaches [7] have been extensively studied.

Machine Learning-Based Interference Mitigation. Recent research has explored AI techniques to dynamically predict and mitigate interference. Du et al. [25] proposed an Interference Neutralization (IN) scheme using

Category	References
Channel Estimation	Song et al. (2023) [20], Gu et al. (2022) [16], Haq et al. (2022) [19], Li et al. (2023) [17], Santos Sousa et al. (2023) [10], Dayi (2022) [12], Shawqi et al. (2023) [24]
Deep Learning	Ozpoyraz et al. (2022) [6], Boas et al. (2022) [7], Shammaa et al. (2023) [8], Doshi et al. (2022) [9], Fang et al. (2022) [13], Sun et al. (2023) [18]
Interference Management	Jeon et al. (2014) [11], Du et al. (2019) [25], Aquilina (2017) [26], Shomorony et al. (2014) [21], Yang et al. (2016) [27], Sridharan (2015) [28]
Full-Duplex Systems	Chae et al. (2017) [29], Jeon et al. (2015) [30], Du et al. (2019) [25], Aquilina (2017) [26], Jeon et al. (2014) [31]
PRACH Preamble Design	Xiong et al. (2018) [15], Schreiber et al. (2018) [14], Fang et al. (2022) [13], Launay (2022) [32]
PUSCH Uplink Coverage Enhancement	Guo et al. (2020) [33], Demirsoy et al. (2009) [34]
Machine Learning for Wireless Networks	Shawqi et al. (2023) [24], Santos Sousa et al. (2023) [10], Doshi et al. (2022) [9]
Network Architecture and Optimization	Dahlman et al. (2020) [1], Bertenyi et al. (2018) [2], Ahmadi (2019) [4], Parkvall et al. (2020) [3], Morais (2023) [35]
Interference Neutralization	Du et al. (2019) [25], Kannan et al. (2011) [36], Aquilina (2017) [26]

Table 1. Taxonomy of PRACH and PUSCH Interference Management Related Works

Method	Key Benefits	Weaknesses	References
Traditional Channel Estimation	Low complexity, well-established	Limited performance in complex environments with interference	Jeon et al. (2014) [11]
Least Squares (LS) Estimation	Simple implementation, low computational cost	High sensitivity to noise, poor performance in fading channels	Gu et al. (2022) [16]
Minimum Mean Square Error (MMSE) Estimation	Improved performance over LS, reduces noise impact	Requires accurate channel statistics, computationally intensive	Li et al. (2023) [17]
Deep Learning-Based Estimation	High accuracy, adaptive to channel variations	High computational complexity, large dataset requirement	Haq et al. (2022) [19]
GAN-Based Channel Estimation	Superior noise robustness, data-driven learning	Training instability, requires high-quality labeled data	Doshi et al. (2022) [9]
Manifold Learning-Based Estimation	Efficient for high-dimensional mmWave channels	Limited interpretability, high memory requirements	Gu et al. (2022) [16]
Reinforcement Learning-Based Estimation	Dynamic adaptation to changing environments	Requires extensive training, sensitive to hyperparameters	Boas et al. (2022) [7]
Extreme Learning Machine (ELM)	Fast training, good generalization	May not generalize well in highly dynamic environments	Song et al. (2023) [20]

Table 2. Comparison of Channel Estimation Techniques

partial Channel State Information at the Transmitter (CSIT), which significantly reduces inter-user interference. Reinforcement learning-based methods [27] optimize resource allocation, minimizing co-channel interference.

3.4. Full-Duplex Systems

Full-duplex (FD) systems enable simultaneous transmission and reception on the same frequency, theoretically doubling network capacity. However, they suffer from severe self-interference, requiring advanced cancellation techniques.

Comparison with Prior Research. Chae et al. [29] studied self-interference cancellation, proposing a scheme to maximize Degrees of Freedom (DoF) in FD networks. Jeon et al. [30] further analyzed the performance of FD systems under different interference scenarios.

AI-Based Interference Cancellation. Deep learning-based interference suppression methods [8] outperform traditional linear cancellation, dynamically adapting to varying interference levels. These models, however, require extensive real-time processing power, limiting their deployment in mobile networks.

4. Research Methodology

The research methodology used in this study involved evaluating and analyzing 5G-NR PRACH and PUSCH performance in the context of intra-cell and inter-cell interference using the simulation tool Matlab [37]. The simulation framework and setup parameters are presented in detail to provide insights into the conducted experiments and assessments. Additionally, the considerations for both intra-cell and inter-cell interference, which are pivotal in accurately representing real-world scenarios, are discussed.

4.1. PRACH Simulation Setup Parameters

In this study, we rely on MATLAB [37] to simulate and evaluate the 5G-NR Physical Random Access Channel (PRACH). This choice provides a flexible environment for modeling PRACH proceduresÂŮincluding signal generation, channel propagation, and interference modelingÂŮwhile allowing us to precisely control parameters that mirror real-world deployments. Tables 6, 7, and 5 summarize the user equipment (UE) configurations, PRACH setup, and channel properties used in our simulations.

Cyclic Correlation Indices in PRACH. A key aspect of PRACH configuration lies in the *Cyclic Shift Index (CyclicShiftIdx)* and *Root Sequence Index (SeqIdx)*, which determine how ZadoffÂŰChu (ZC) sequences are generated for random access attempts. Specifically, the Root Sequence Index selects the base ZC sequence, and the Cyclic Shift Index is used to generate orthogonal or quasi-orthogonal preamble sequences by cyclically shifting the chosen root sequence. This mechanism allows multiple UEs to transmit random access preambles simultaneously while maintaining a low collision probability. In practice, high-traffic cells often require more extensive root sequences and higher numbers of cyclic shifts to accommodate multiple UEs seeking random access.

Justification of Parameters and Real-World Variation.

- Number of UL Resource Blocks (NULRB): We set this to 6 to reflect a small system bandwidth for proof-of-concept simulations. In commercial deployments, NULRB can range up to hundreds, depending on the frequency band and bandwidth requirements.

- DuplexMode (FDD) and CyclicPrefixUL (Normal): These choices align with typical sub-6 GHz deployments, where frequency-division duplex and a normal cyclic prefix are standard. In millimeter-wave (mmWave) deployments or high-speed scenarios, one might adopt time-division duplexing or extended cyclic prefixes.

- HighSpeed = 0: This indicates normal operation rather than high-speed mobility optimization. Real networks serving high-speed trains or vehicles may enable specialized PRACH formats (e.g., extended CP) to handle rapid channel variations.

- FreqOffset = 0: We assume no carrier frequency offset in the simulation. In reality, frequency offsets can arise from hardware imperfections or Doppler shifts; operators often introduce offset compensation to prevent performance degradation.

- PreambleIdx and CyclicShiftIdx: These parameters enable multiple orthogonal preambles in a single cell. Higher-index values and varied cyclic shifts reduce collisions when many UEs attempt random access simultaneously. Dense urban cells with heavy uplink contention often require more preamble resources.

4.2. PUSCH Simulation Setup Parameters

In this study, we evaluate the 5G-NR Physical Uplink Shared Channel (PUSCH) to understand how intra-cell and inter-cell interference affects uplink throughput, latency, and reliability. The simulation environment, built upon the Matlab 5G-NR toolbox [37], provides built-in functionality for generating, processing, and analyzing PUSCH signals under realistic propagation conditions. Tables 6 and 7 outline the main configuration parameters for user equipment (UE) and PUSCH transmission mode, respectively.

Technical Concepts of PUSCH. The PUSCH is the primary channel used by UEs to transmit user data and control information in the uplink. Key elements influencing its performance include:

- Modulation and Coding Scheme (MCS): Determines how bits are mapped to modulation symbols (e.g., 64-QAM) and the coding rate applied for error correction. A higher-order modulation (e.g., 64-QAM) can boost throughput but is more sensitive to noise and interference.

- HARQ (Hybrid Automatic Repeat reQuest): Provides retransmission of erroneously received data. The parameters *NBundled*, *BetaCQI*, *BetaRI*, and *BetaACK* manage overhead for HARQ-ACK, channel quality (CQI), and rank indication (RI) feedback. Tuning these values influences both reliability and uplink overhead.

	Target UE (T-UE)	Interfering UE (I-UE)	Description
NULRB	6	6	Number of UL Resource Blocks (RB)
DuplexMode	FDD	FDD	Frequency Division Duplex (FDD)
CyclicPrefixUL	Normal	Normal	Normal cyclic prefix (CP)
NTxAnts	1	1	Number of transmit antennas

Table 3. User Equipment (UE) Configuration

	PRACH Config (Target UE)	PRACH Config (Interf. UE)	Description
Format	0	0	PRACH format (TS36.104, Table 8.4.2.1-1)
SeqIdx	22	[0, 1, 2, 3, 4, 22]	Root Sequence Index (ZC base sequence)
CyclicShiftIdx	1	1	Cyclic shift index for preamble separation
HighSpeed	0	0	Normal mode (no extended CP for high speed)
FreqOffset	0	0	Default carrier frequency offset
PreambleIdx	32	[0, 3, 37, 42, 63]	Distinguishes random-access preambles

Table 4. PRACH Configuration

	Channel Configuration	Description
NRxAnts	2	Number of receiving antennas
DelayProfile	ETU	Extended Typical Urban delay profile
DopplerFreq	70 [Hz]	Doppler frequency for mobility
MIMOCorrelation	Low	Correlation level among MIMO antenna ports
Seed	1	Random seed for channel generation
NTerms	16	Number of oscillators in fading model
ModelType	GMEDS	Rayleigh fading model type
InitPhase	Random	Random initial phases for fading
NormalizePathGains	On	Normalizes power across channel paths
NormalizeTxAnts	On	Ensures consistent transmit power

Table 5. Propagation Channel Configuration

- Resource Blocks and PRBSet: Defines the specific frequency-domain resources allocated to the UE. In dense deployments, operators may dynamically assign fewer or more resource blocks based on real-time interference and throughput demands.

Choice of Simulation Parameters and Real-World Variations.

- NCellID: We use distinct NCellID values to separate cells (e.g., 100 vs. [20, 90, 110]), effectively modeling multi-cell interference scenarios. In practice, operators assign unique cell IDs in contiguous frequency bands to minimize confusion between neighboring cells.

- DuplexMode (FDD) and CyclicPrefixUL (Normal): These settings reflect common sub-6 GHz deployments, where FDD is widely adopted and a

Normal CP suffices. In TDD or mmWave deployments, an Extended CP may be needed to combat severe multipath.

- NTxAnts: A single transmit antenna is assumed (NTxAnts=1) for clarity in this study, but commercial devices commonly employ multiple antennas and transmit diversity to counteract fading, especially in higher frequency bands.
- Shortened=0: A full-length subframe is used in our simulation. In certain low-latency or specialized applications, a shortened subframe could reduce turnaround times, albeit with less effective channel estimation.
- Modulation (64-QAM): We assume 64-QAM to represent a moderate-to-high data rate scenario. In reality, lower modulation (QPSK, 16-QAM) might be used in coverage-limited areas, while higher modulation (256-QAM) may be employed under favorable conditions.
- NTurboDecIts=5: This parameter specifies the number of turbo decoder iterations to balance error correction performance against decoding complexity. Network operators can adjust turbo or LDPC decoder iterations dynamically based on throughput and latency requirements.
- HARQ and Feedback Parameters: The parameters *NBundled*, *OCQI*, *ORI*, *OACK*, and Beta values control how user feedback is encoded and sent. In real networks, these may be dynamically tuned to accommodate changing traffic loads and interference levels.

Although our chosen parameter set is intentionally constrained to simplify analysis, real-world implementations may vary considerably depending on cell density, carrier frequency, and user mobility patterns. For instance, extended bandwidth deployments (e.g., 100 MHz in mmWave bands) often require advanced scheduling algorithms and adaptive MCS to mitigate severe path loss and fluctuating interference.

4.3. Intra-Cell and Inter-Cell Interference Considerations

In the realm of 5G-NR communication, the presence of intra-cell and inter-cell interference is a critical aspect that demands meticulous consideration. We modeled these interferences within our Matlab simulator [37] to ensure the accuracy and reliability of our simulation outcomes.

Intra-Cell and Inter-Cell Interference Simulation for PRACH. The following subsections describe the specific configurations and approaches used to simulate the intra-cell and inter-cell interference for PRACH in the Matlab simulator [37].

(1) *Intra-Cell Interference*: Intra-cell NR-PRACH interference are modeled in the Matlab simulator [37] using an 'Interfering" UE (i.e., the UE generating the interference) with the same UE configuration (refer to Table 6) and the same PRACH configuration (refer to Table 6), except for the Preamble Index", which differs from whose of the Target UE" (T-UE). This scenario is exemplified by Interfering" UE_1 $(I - UE_1)$ in Figure 3.

(2) *Inter-Cell Interference*: In the case of NR-PRACH inter-cell interference, it is modeled using a 'Interfering" UE that shares the same UE configuration (refer to Table 6) and the same PRACH configuration (refer to Table 7) with the Target" UE with the exception of the Logical sequence index" or root sequence index", which differs from whose of the target" UE. It corresponds to the Interfering" UE_2 and Interfering" UE_3 of Figure 3. In fact, in a 5G-NR cell, all UEs within the cell share the same Logical Sequence Index" or Root Sequence Index," while the UEs themselves are differentiated from each other using a Preamble Index". The parameter Logical Sequence Index" or Root Sequence Index" serves to distinguish 5G-NR cells from one another. For example Target" UE (T-UE) and Interfering" UE_1 of Figure 3 are sharing the same Logical Sequence Index" or Root Sequence Index but they have different Preamble Index" for Random-Access (RA).

Intra-Cell and Inter-Cell Interference Simulation for PUSCH. The following subsections describe the specific configurations and approaches used to simulate the intra-cell and inter-cell interference for PUSCH in the Matlab simulator [37].

(1) Intra-Cell Interference: In the Matlab simulator [37], intra-cell NR-PUSCH interference is modeled using an 'Interfering" UE (i.e., the UE generating the interference) with the same UE configuration (refer to Table 6) and the same PUSCH configuration (refer to Table 7), except for the RNTI, which differs from that of the Target UE" (T-UE). This scenario is exemplified by Interfering" UE_1 $(I - UE_1)$ in Figure 6.

(2) Inter-Cell Interference: In the case of NR-PUSCH inter-cell interference, it is modeled using an 'Interfering" UE that shares the same UE configuration (refer to Table 6) and the same PUSCH configuration (refer to Table 7) with the Target" UE, except for the NCellID", which differs from that of the Target" UE. This corresponds

Parameters	Target Mobile	Interfering Mobile	Description
NCellID	100	[20, 90, 110]	Cell identification ID
DuplexMode	FDD	FDD	Frequency Division Duplexing (FDD)
CyclicPrefixUL	Normal	Normal	Normal cyclic prefix (CP)
NTxAnts	1	1	Number of transmission antennas
Shortened	0	0	Option to shorten the subframe by omitting the last symbol
RNTI	1	[20, 33, 57, 68]	Mobile identification ID
Hopping	Off	Off	PUSCH frequency hopping
SeqGroup	0	0	The sequence group

Table 6. UE Configurations for PUSCH

Parameters	Values	Description
NLayers	1	Physical layer process for PUSCH transmission
TxScheme	"Port0"	PUSCH transmission schemes (Codebook and non-codebook based)
Modulation	"64-QAM"	PUSCH modulation scheme used
NTurboDecIts	5	Number of turbo decoder iteration cycles
PRBSet	(0: NULRB-1)	Set of PRBs used for data transmission on PUSCH
NBundled	0	HARQ-ACK bundling sequence index
OCQI	0	Number of uncoded channel quality information (CQI) bits
ORI	0	Number of uncoded Rank Indication (RI) bits
OACK	0	Number of uncoded ACK bits
BetaCQI	2	MCS offset for CQI and PMI bits
BetaRI	3	MCS offset for RI bits
BetaACK	1	MCS offset for HARQ-ACK bits

Table 7. PUSCH Transmission Mode Configuration

to the Interfering" UE_2 and Interfering" UE_3 in Figure 6. In a 5G-NR cell, all UEs within the cell share the same NCellID", while the UEs themselves are differentiated from each other using a RNTI". The NCellID" parameter serves to distinguish 5G-NR cells from one another. For example, the Target" UE (T-UE) and Interfering" UE_1 in Figure 6 share the same NCellID" but have different RNTI" for PUSCH Transmission and Reception.

4.4. AI and Machine Learning for Adaptive Interference Management

Recent advancements in AI and machine learning have shown promise in adaptive interference management. Reinforcement learning techniques [7] have been used to dynamically allocate resources and mitigate interference. Deep learning-based channel estimation [19] improves signal detection accuracy in real-time, and GAN-based models [9] enhance noise resilience.

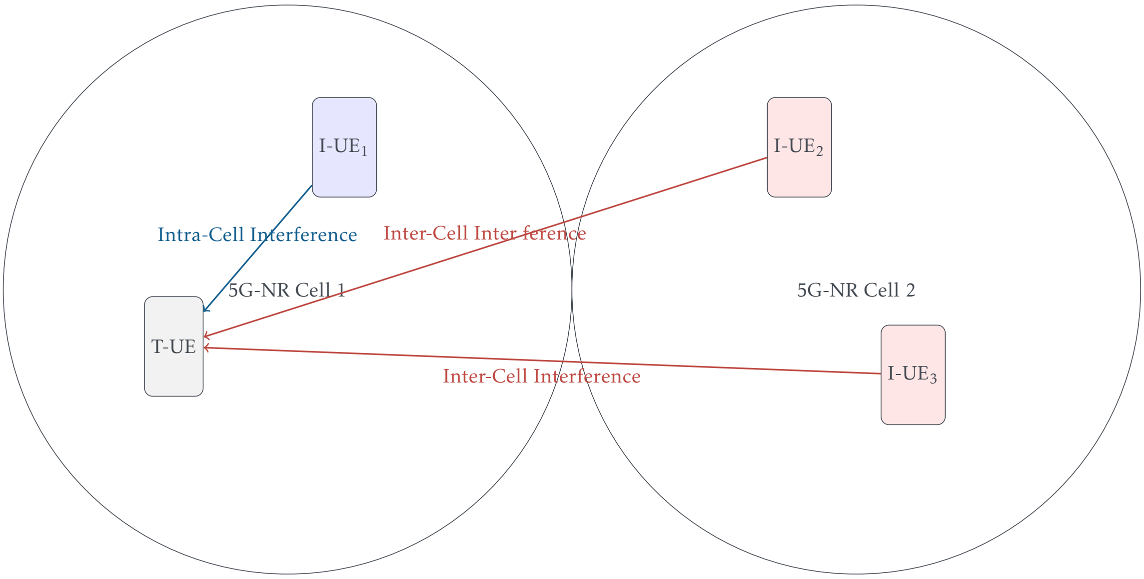

Figure 6. Intra-Cell and Inter-Cell Interference in 5G-NR PUSCH Scenario.

Method	Key Benefits	Weaknesses	References
Traditional Channel Estimation	Low complexity, well-established	Limited adaptability	Jeon et al. (2014) [11]
Deep Learning-Based Estimation	High accuracy, adaptive to variations	High computational cost	Haq et al. (2022) [19]
GAN-Based Channel Estimation	Superior noise robustness	Requires large training datasets	Doshi et al. (2022) [9]
Reinforcement Learning-Based Estimation	Dynamic adaptation to interference	Complex training process	Boas et al. (2022) [7]

Table 8. Comparison of AI-Based Channel Estimation Techniques

This study explores how integrating AI-driven techniques with existing interference management strategies can significantly enhance 5G-NR network performance.

5. Results and Discussion

In this section, we present and analyze the performance results of NR-PRACH and NR-PUSCH under varying conditions of intra-cell and inter-cell interference. The simulations were conducted to evaluate the robustness of these key 5G NR components in scenarios reflecting realistic network deployments. The results are discussed in detail with a focus on how different configurations of Preamble Index, RootSequenceIndex and RNTI affect the Correct Detection Rate (CDR) for NR-PRACH and the Block Error Rate (BLER) for NR-PUSCH. The discussion also links these findings back to the simulation models and methodologies offering insights into the underlying factors that drive the observed performance trends. This analysis is crucial for understanding the interference management challenges in 5G networks and for identifying potential optimization strategies to enhance network reliability and efficiency.

5.1. Performance of NR-PRACH under Conditions of Intra-Cell Interference

The performance of NR-PRACH was evaluated using the Correct Detection Rate (CDR) or Preamble Detection Probability, calculated over 1000 subframes. The intra-cell interference was modeled by introducing an "Interfering" UE (I-UE) within the same cell as the "Target" UE (T-UE). Both UEs shared the same "Logical Sequence Index" but used different "Preamble Index" values.

The modeling of intra-cell interference in this study was crucial to simulate realistic network scenarios where multiple UEs operate within the same cell but are distinguished by their preamble indices. This approach aligns with expected real-world behavior, where such interference is a common challenge in densely populated cells.

Figures 7 and 8 present the performance of PRACH under varying levels of intra-cell interference with the

RootSequenceIndex set to 22 for different Preamble Index values. The results are designed to assess the robustness of PRACH as the Preamble Index of the Interfering UE changes. It is important to note that the Preamble Index of the Target UE was fixed at 32 in all simulations for consistency.

The results shown in Figures 7 and 8 indicate that NR-PRACH performance, specifically the preamble detection probability, decreases as the intra-cell interference level increases (i.e., as the SNRdB value of the I-UE increases). This outcome is expected, as higher interference levels typically result in more significant challenges for accurate preamble detection.

Additionally, the results demonstrate that the degradation in PRACH performance occurs regardless of the specific Preamble Index used by the Interfering UE. This suggests that intra-cell interference has a general adverse effect on PRACH, independent of the particular preamble index being used.

Figures 9 and 10 further explore the performance of PRACH under intra-cell interference by varying the Preamble Index values while maintaining a constant level of interference. The goal here is to identify which Preamble Index values allow the Target UE to better withstand intra-cell interference.

The findings from these figures reveal that at a relatively low level of intra-cell interference (SNRdB [I-UE] = -27dB, see Figure 9), the performance of NR-PRACH remains stable regardless of the Preamble Index values used by the Interfering UE. However, as the interference level increases to a moderate level (SNRdB [I-UE] = -23dB, see Figure 10), NR-PRACH performance becomes sensitive to the specific Preamble Index values employed by the Interfering UE. This sensitivity indicates that certain Preamble Index values may be more robust against interference than others under higher interference conditions.

In operational networks, random access preambles are typically assigned in bulk, and individual Preamble Index selection is not dynamically optimized per UE. Nonetheless, these results imply that careful dimensioning of preamble sets can help mitigate collisions in scenarios with high device density and persistent interference.

5.2. Performance of NR-PRACH under Conditions of Inter-Cell Interference

The performance of NR-PRACH under inter-cell interference was also evaluated using the Correct Detection Rate (CDR) over 1000 subframes. In this scenario, the inter-cell interference was simulated by placing the "Interfering" UE in a neighboring cell to the Target UE's cell. The Interfering UE used a different "Logical Sequence Index" but could potentially share the same "Preamble Index" as the Target UE.

This modeling approach effectively captures the challenges faced in multi-cell environments where overlapping signals from adjacent cells can interfere with PRACH performance. Such conditions are critical to consider in evaluating the resilience of NR-PRACH in practical deployments.

Figures 11 and 12 illustrate the performance of PRACH in the presence of inter-cell interference, with the Target UE having a RootSequenceIndex of 22, while the Interfering UE uses RootSequenceIndex values of 0 and 4, respectively, and a Preamble Index value of 3.

The results show that the performance of NR-PRACH, in terms of preamble detection probability, deteriorates as the level of inter-cell interference increases (i.e., as the SNRdB value of the Interfering UE increases). This trend is consistent with the findings from the intra-cell interference simulations and aligns with expectations that higher interference levels generally impair detection accuracy.

Moreover, the degradation in PRACH performance is observed regardless of the RootSequenceIndex value used by the Interfering UE, suggesting that inter-cell interference similarly impacts PRACH performance, independent of specific root sequence assignments.

Figures 13 and 14 further analyze PRACH performance by varying the RootSequenceIndex values of the Interfering UE while keeping the inter-cell interference level constant. The purpose is to determine which RootSequenceIndex values offer better resilience to inter-cell interference for the Target UE.

The results indicate that at a lower level of inter-cell interference (SNRdB [I-UE] = -24dB, refer to Figure 13), the performance of NR-PRACH remains relatively consistent across different RootSequenceIndex values. However, as the interference level increases (SNRdB [I-UE] = -9dB, refer to Figure 14), the performance of NR-PRACH becomes more sensitive to the specific RootSequenceIndex values used by the Interfering UE. For example, a RootSequenceIndex of 1 was found to significantly degrade PRACH performance compared to a RootSequenceIndex of 4, indicating that some sequence indices may be more susceptible to interference than others under high-interference conditions.

Although 3GPP standards typically fix RootSequenceIndex allocations per cell, networks with adaptable or reconfigurable preamble resources might reduce cross-cell interference via sequence planning. Especially in urban macro deployments or multi-layer (macro/femto/pico) networks, dynamic assignment of root sequences could alleviate congestion hot spots.

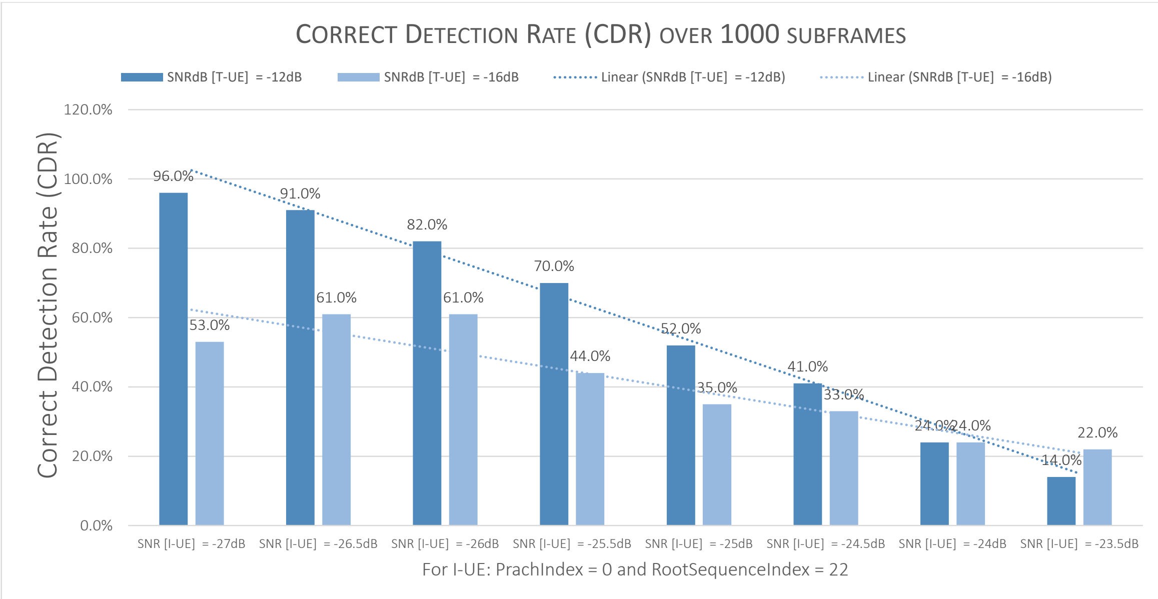

Figure 7. 5G-NR PRACH Performance in the Presence of Intra-Cell Interference with Preamble Index = 0 and Root Sequence Index = 22

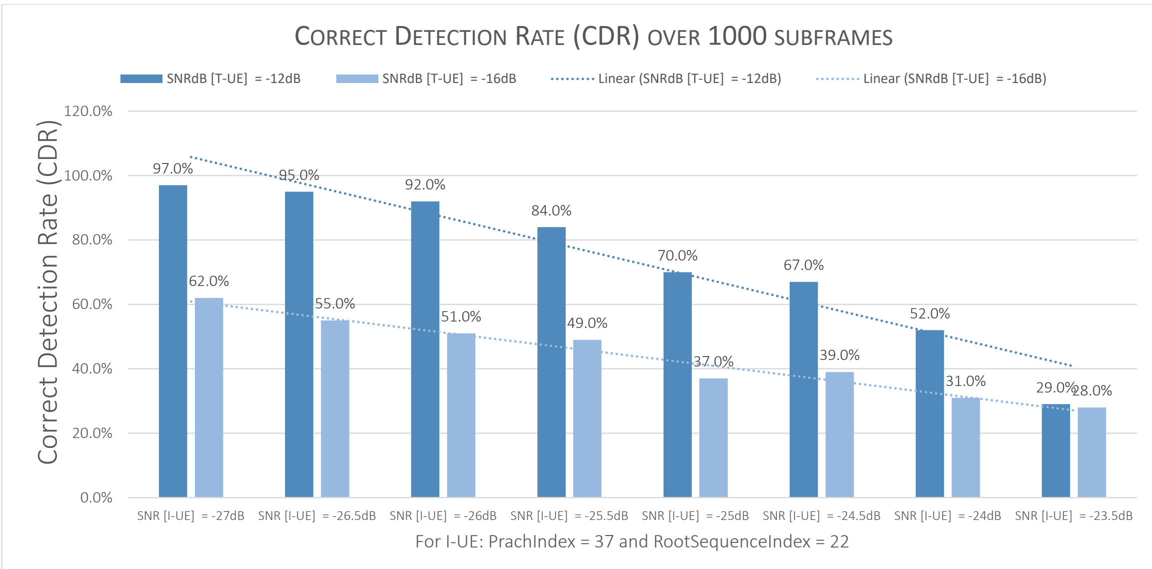

Figure 8. 5G-NR PRACH Performance in the Presence of Intra-Cell Interference with Preamble Index = 37 and Root Sequence Index = 22

5.3. Performance of NR-PUSCH under conditions of intra-cell interference

The performance of NR-PUSCH is evaluated using the Block Error Rate (BLER) over 1000 PUSCH data blocks. Intra-cell interference is simulated with an UE in the same cell as the target UE (Target UE), sharing the same NCellID but using a different RNTI. Figure 15, Figure 16, Figure 17 and Figure 18 present the PUSCH performance under intra-cell interference (NCellID = 100) for different RNTI values (20, 33, 57 and 68). The aim is to assess the robustness of PUSCH relative to the interfering UE's RNTI value. The simulations have been run by using a RNTI set 1 for the Target UE.

Figure 15 (RNTI = 20) shows a significant dependency of BLER on SNR values. At the lowest SNR of -2.5 dB, BLER reaches nearly 100% (0.998). This indicates an extremely poor reception quality. As the SNR improves to -2 dB and further to -1 dB, there is a significant decrease in BLER to 18.7% and 0.7% respectively. This demonstrates a clear inverse correlation between SNR and BLER, where higher SNR values substantially improve reception quality.

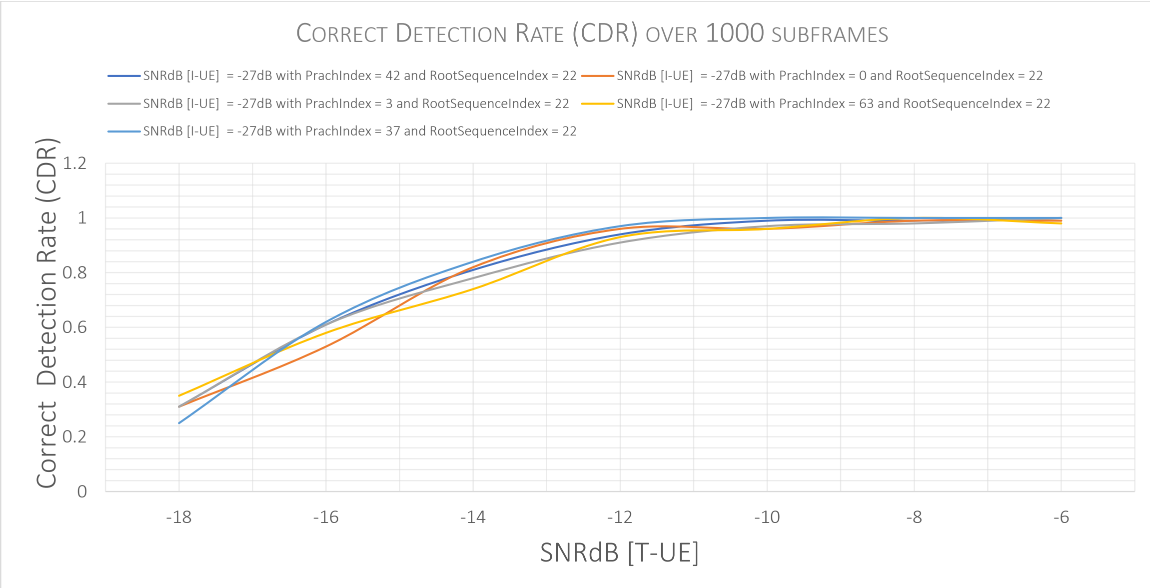

Figure 9. PRACH Performance in presence of Intra-Cell Interference with a Root Sequence Index of 22 and SNRdB [I-UE] of -27 dB for various "Preamble Index" values.

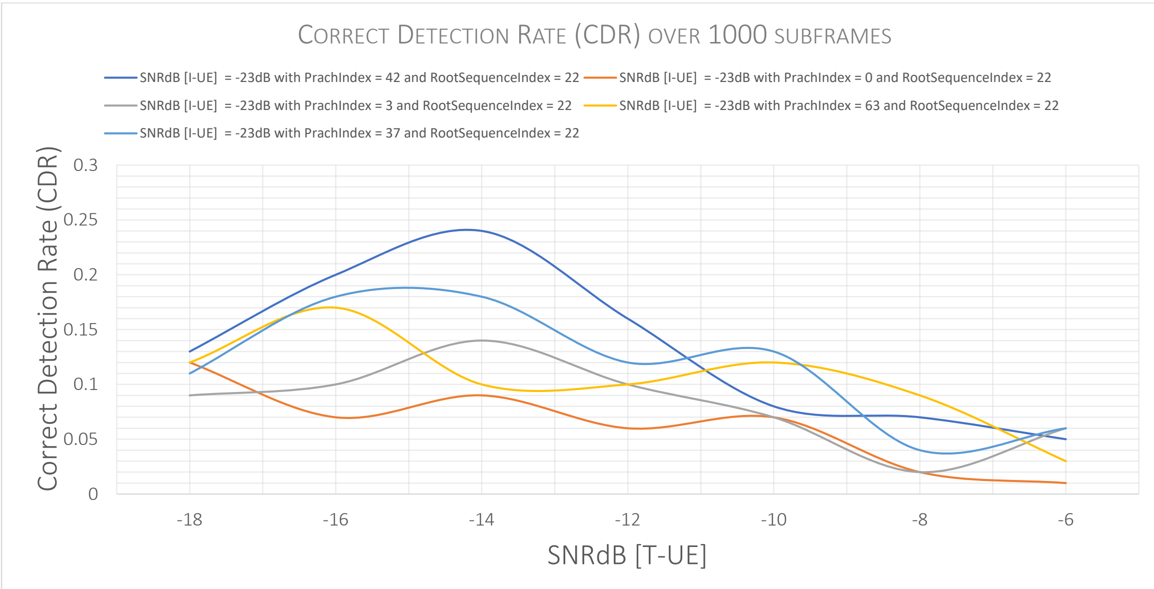

Figure 10. PRACH Performance in presence of Intra-Cell Interference with a Root Sequence Index of 22 and SNRdB [I-UE] of -23 dB for various "Preamble Index" values.

Figure 16 (RNTI = 33) shows similar trends as Figure 15 where BLER decreases with the increase in SNR. When Target UE operates at SNR of -2 dB and better, the effects of intra-cell interference are considerably mitigated. This suggests that the RNTI configured at 33 has better inherent resistance to the intra-cell interference.

In Figure 17 (RNTI = 57), there is consistent improvement in BLER with increasing SNR levels. At the highest SNR tested (-1 dB) for Target UE, BLER approaches 0%; this indicates the optimal performance under high SNR conditions despite the presence of intra-cell interference. This suggests effective interference handling or superior signal resilience when RNTI is configured to 57. 18 (RNTI = 68) again shows a significant reduction in BLER as SNR increases, the result achieving near-zero BLER at the highest SNR level.

Comparing the results across the Figure 15, Figure 16, Figure 17 and Figure 18 at an SNR of -2.5 dB and SNRdBInterf = -20 dB with NCellID = 100 is considerably impacted by the noise and interference levels. These conditions are not ideal for PUSCH, as they lead to a higher rate of transmission errors. The

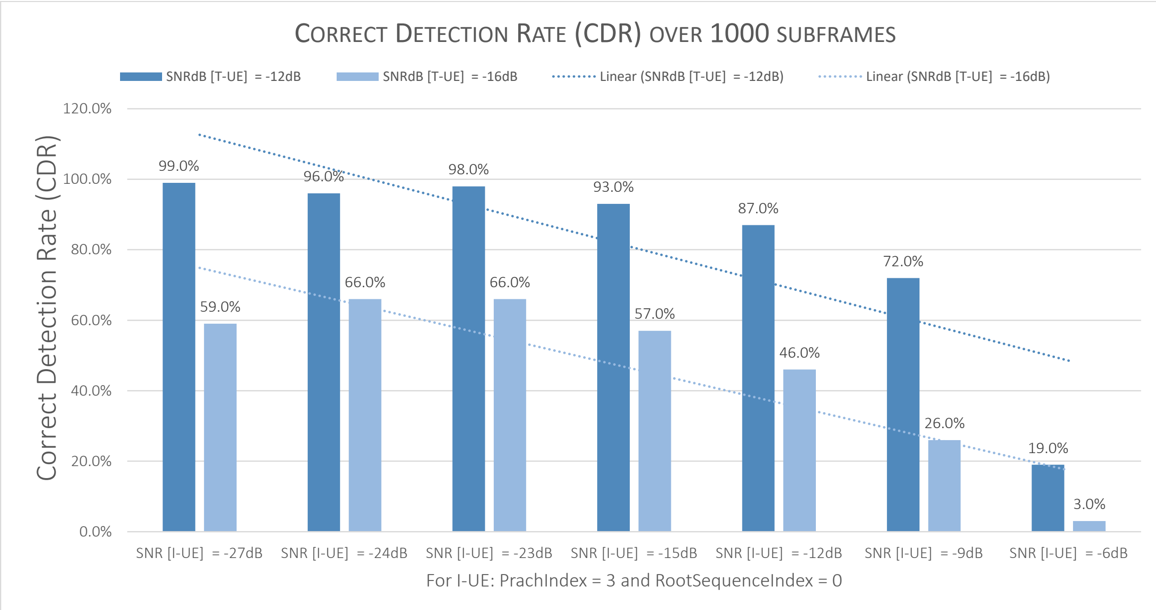

Figure 11. PRACH Performance in the Presence of Inter-Cell Interference with "Preamble Index" = 3 and Root Sequence Index = 0.

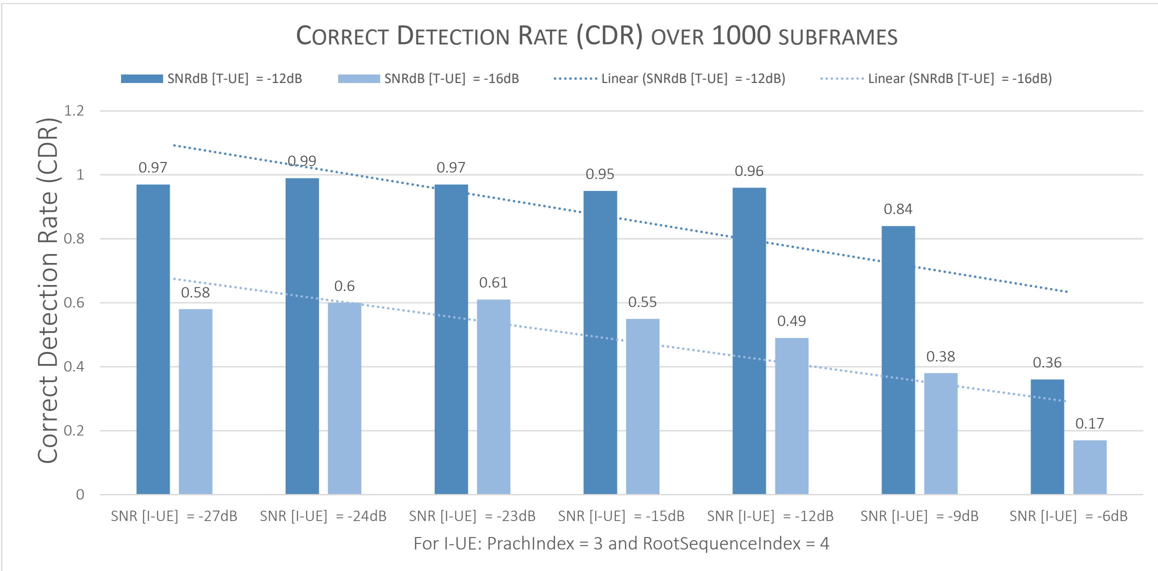

Figure 12. PRACH Performance in the Presence of Inter-Cell Interference with "Preamble Index" = 3 and Root Sequence Index = 4.

PUSCH BLER values are all relatively high (around 17.8%). This suggests that the communication quality at an SNR of -2.5 dB and SNRdBInterf = -20 dB is considerably impacted by the noise and interference levels.

These variations is attributed to RNTI-specific parameters that influence how signals are processed and errors are managed. Understanding these differences is crucial for network engineers and system designers to tailor strategies that enhance the overall robustness and efficiency of the 5G NR-PUSCH systems especially in environments characterized by high levels of interference. The disparity in BLER across different RNTIs under identical testing conditions also suggests that tuning specific parameters related to individual RNTIs could yield significant improvements in performance, particularly for those configurations currently showing higher BLER. This insight could guide targeted interventions to enhance system reliability and throughput in real-world deployments.

In commercial deployments, the base station dynamically assigns RNTIs and configures scheduling intervals. While operators typically do not pick RNTIs for interference control, these findings imply that adaptive

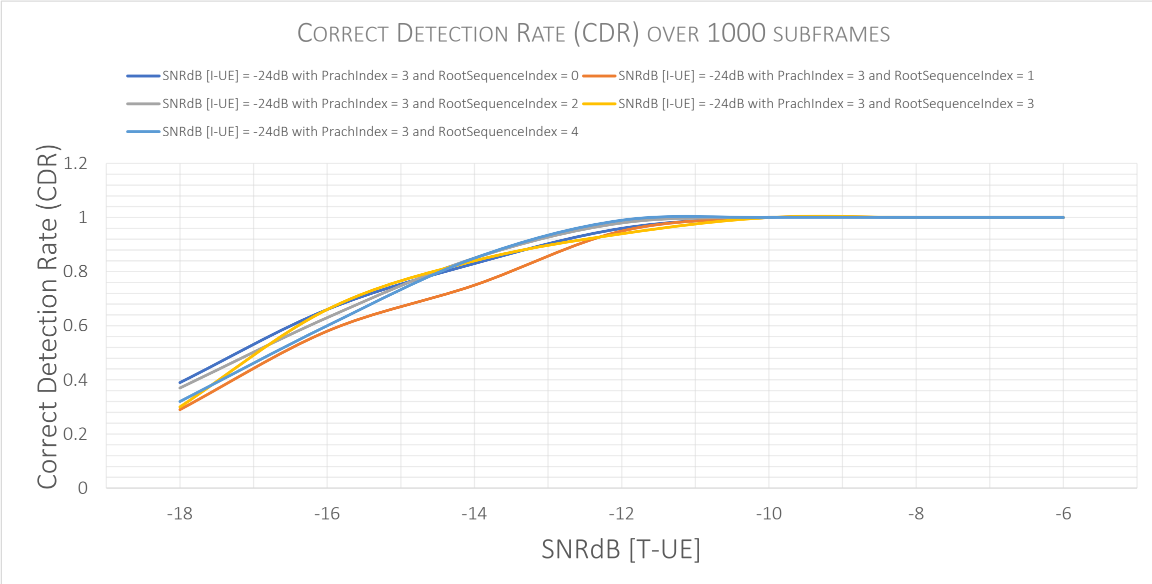

Figure 13. PRACH Performance in the Presence of Inter-Cell Interference with "Preamble Index" = 3 and SNRdB [I-UE] = -24dB for different Values of RootSequenceIndex for the Interfering Cell.

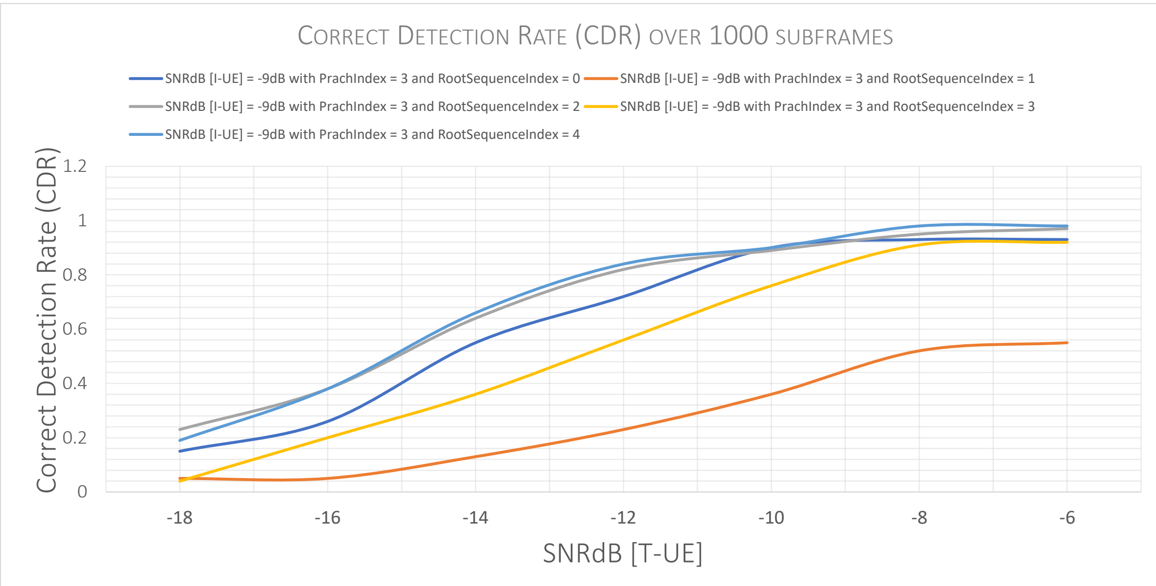

Figure 14. PRACH Performance in the Presence of Inter-Cell Interference with "Preamble Index" = 3 and SNRdB [I-UE] = -9dB for different Values of RootSequenceIndex for the Interfering Cell.

or load-aware RNTI management could incrementally reduce collisions and error rates in heavily loaded cells. Moreover, advanced link adaptation (switching MCS based on real-time interference metrics) remains essential to handle uplink fluctuations effectively.

5.4. Performance of NR-PUSCH under conditions of inter-cell interference

The performance of NR-PUSCH is evaluated through the Block Error Rate (BLER) measured across 1000 PUSCH data blocks. Inter-cell interference is simulated by introducing an UE in a neighboring cell with different "NCellID" values and possibly the same "RNTI" as the target mobile. Figure 19, Figure 20 and Figure 21 show PUSCH performance under inter-cell interference conditions (NCellID = 100 for the Target UE and NCellID = 20, 90 and 110 for the Interfering UE) with RNTI set to 20.

In Figure 19 (NCellID = 20), BLER significantly increases as the SNRdBInterf (Interference from other cells SNR) increaes, moving from -25dB to -10dB. This trend is evident as the interference reduces the quality of the PUSCH reception. At SNRdBInterf = -25dB, even

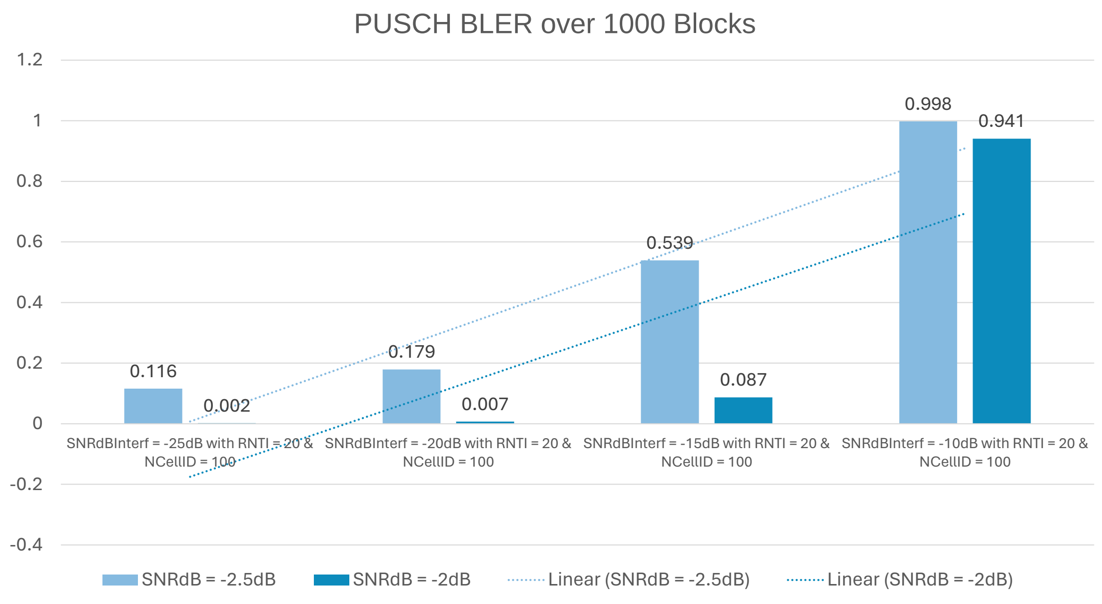

Figure 15. PUSCH BLER for RNTI = 20 with varying SNR and intra-cell interference levels

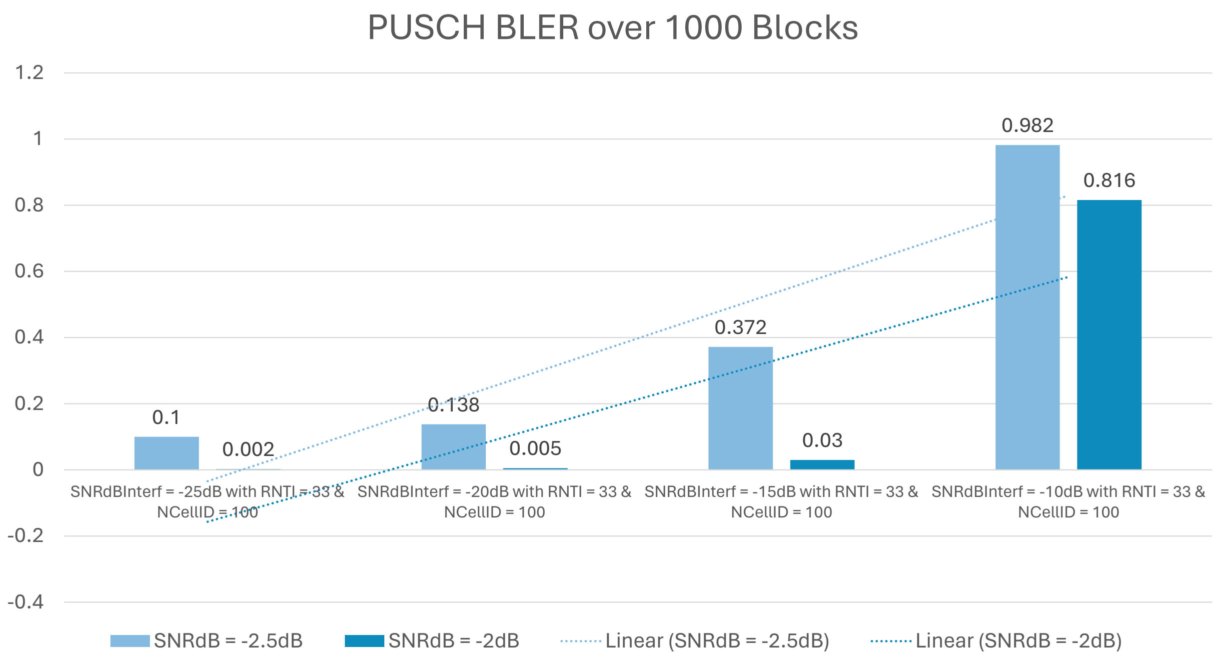

Figure 16. PUSCH BLER for RNTI = 33 with varying SNR and intra-cell interference levels

with the Target UE's SNR at -2.5dB, the BLER remains at a reasonnable level (11.5%). This indicates a robustness against interference. However, as interference increases, PUSCH BLER escalates sharply, reaching nearly 100% (99.4%) at -10dB SNRdBInterf, showcasing extreme susceptibility to higher interference levels.

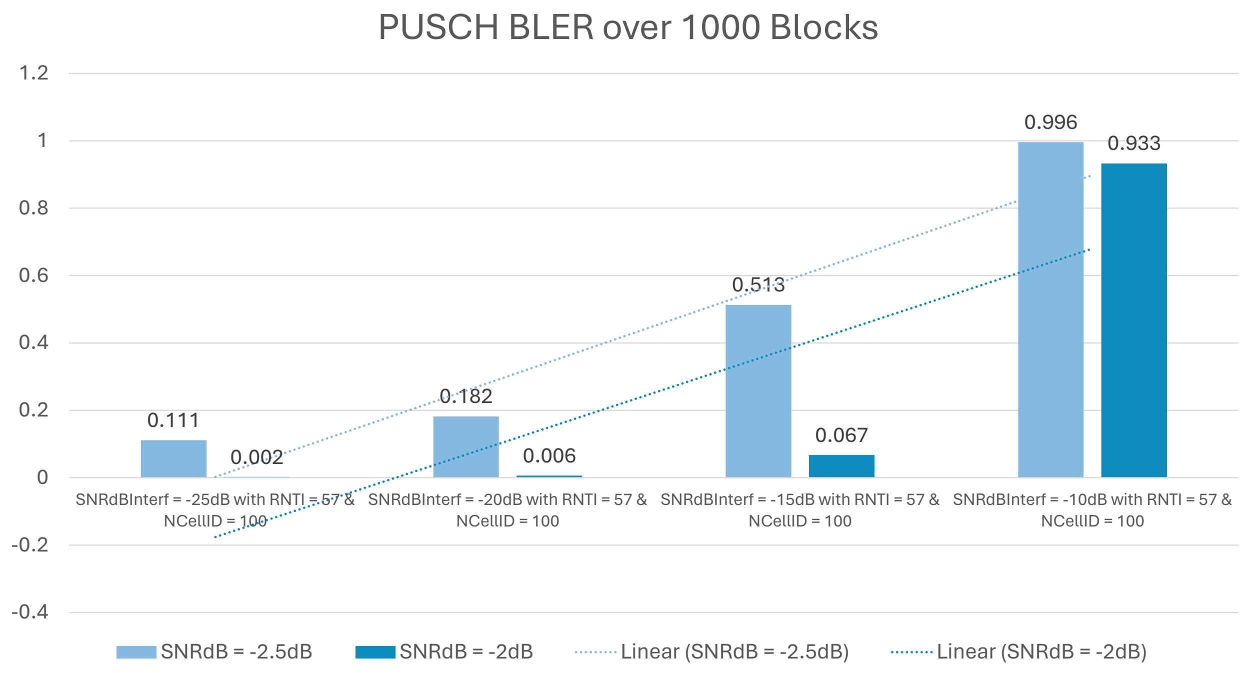

Figure 17. PUSCH BLER for RNTI = 57 with varying SNR and intra-cell interference levels

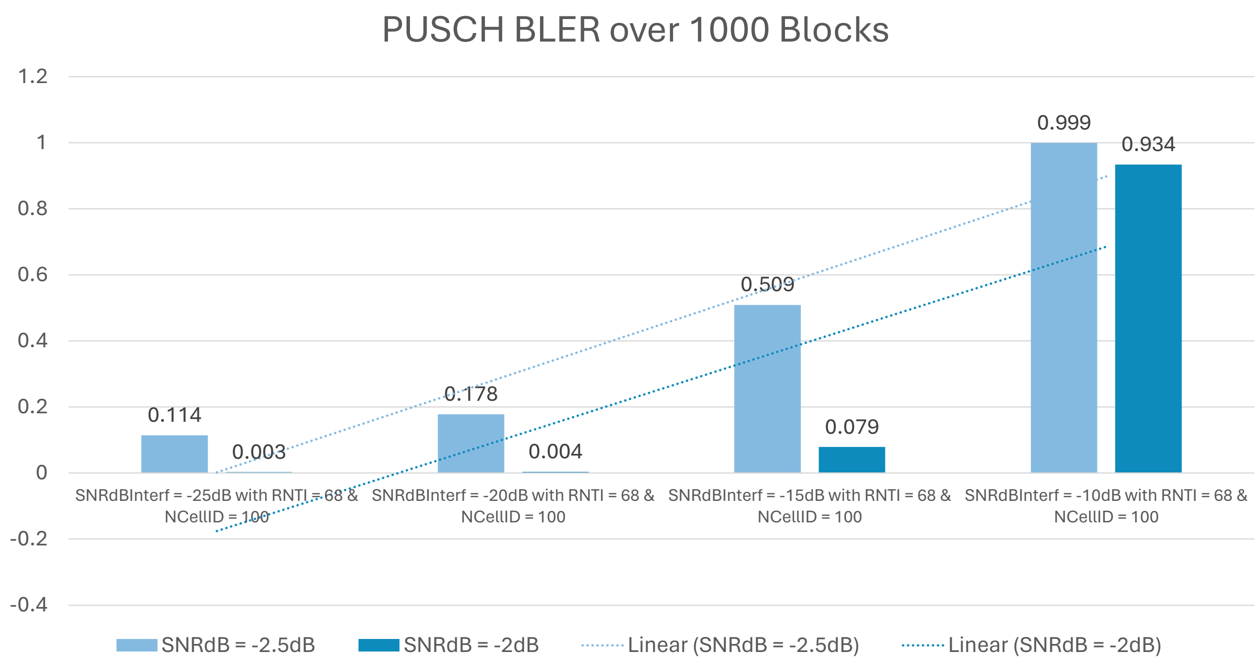

Figure 18. PUSCH BLER for RNTI = 68 with varying SNR and intra-cell interference levels

Similar to Figure 19, Figure 20 (NCellID = 90) shows a progressive worsening of PUSCH BLER as the inter-cell interference increases. The initial PUSCH BLER at -25dB SNRdBInterf starts higher than in Figure 19 (12.5% vs. 11.5%). This suggests that different NCellID configurations might be influencing the sensitivity to intercell-interference.

Again similar to Figure 19, Figure 20, Figure 21 (NCellID = 110) follows a consistent trend where increased inter-cell interference significantly impacts the PUSCH BLER. The PUSCH BLER starts at a slightly higher baseline (10.5%) compared to Figure 19 with NCellID = 20. This indicates possible variations in

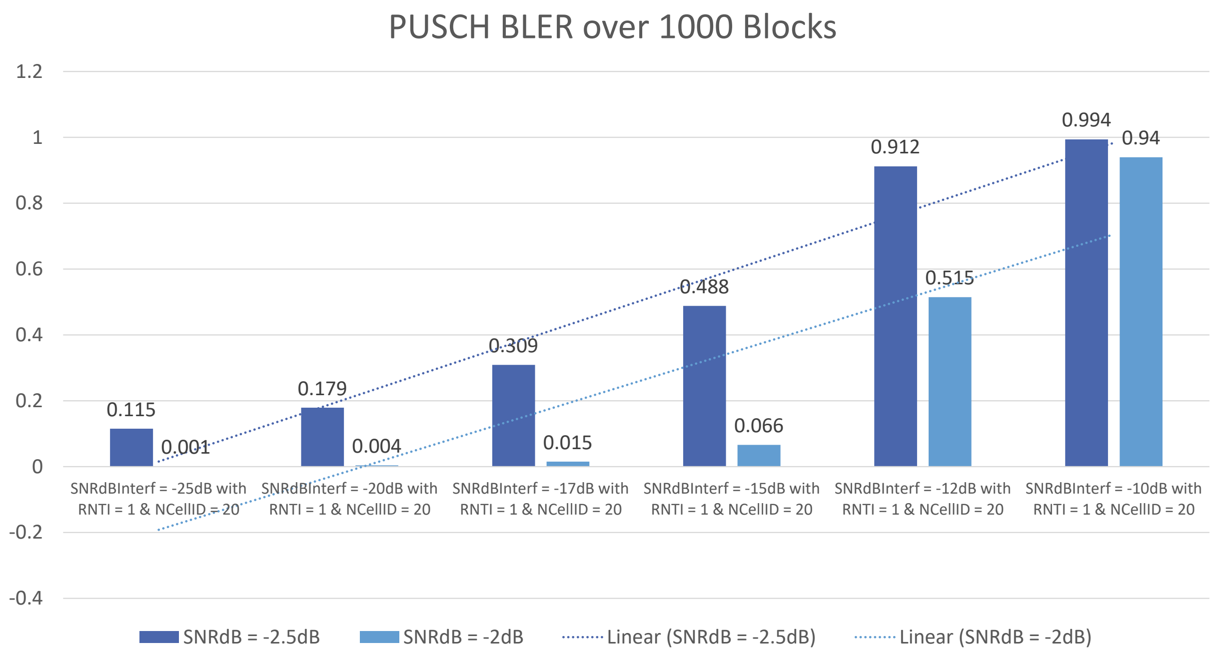

Figure 19. PUSCH BLER for NCellID = 20 with varying SNR and inter-cell interference levels

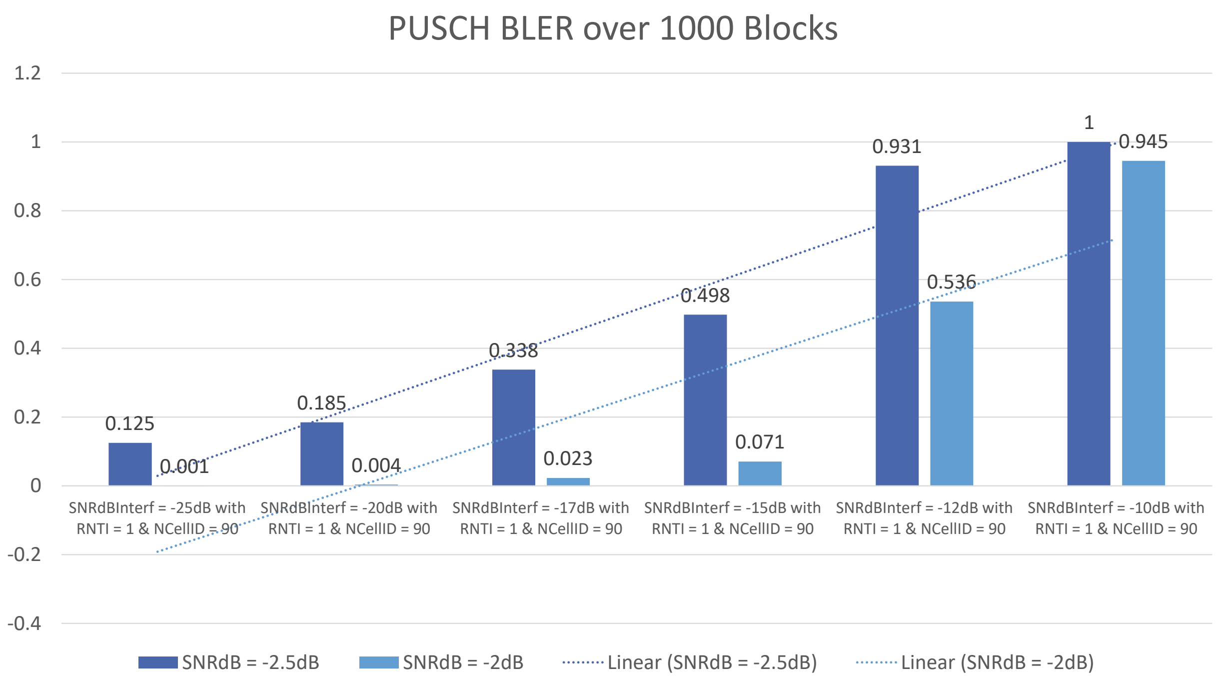

Figure 20. PUSCH BLER for NCellID = 90 with varying SNR and inter-cell interference levels

channel conditions, NCellID configurations, or other parameters affecting PUSCH performance.

Operators commonly employ inter-cell interference coordination (ICIC) or advanced CoMP (Coordinated Multi-Point) approaches to limit simultaneous uplink transmissions on overlapping frequencies. Our simulation corroborates the need for such coordination; otherwise, users in adjacent cells may suffer drastic BLER surges, leading to poor throughput and increased retransmissions.

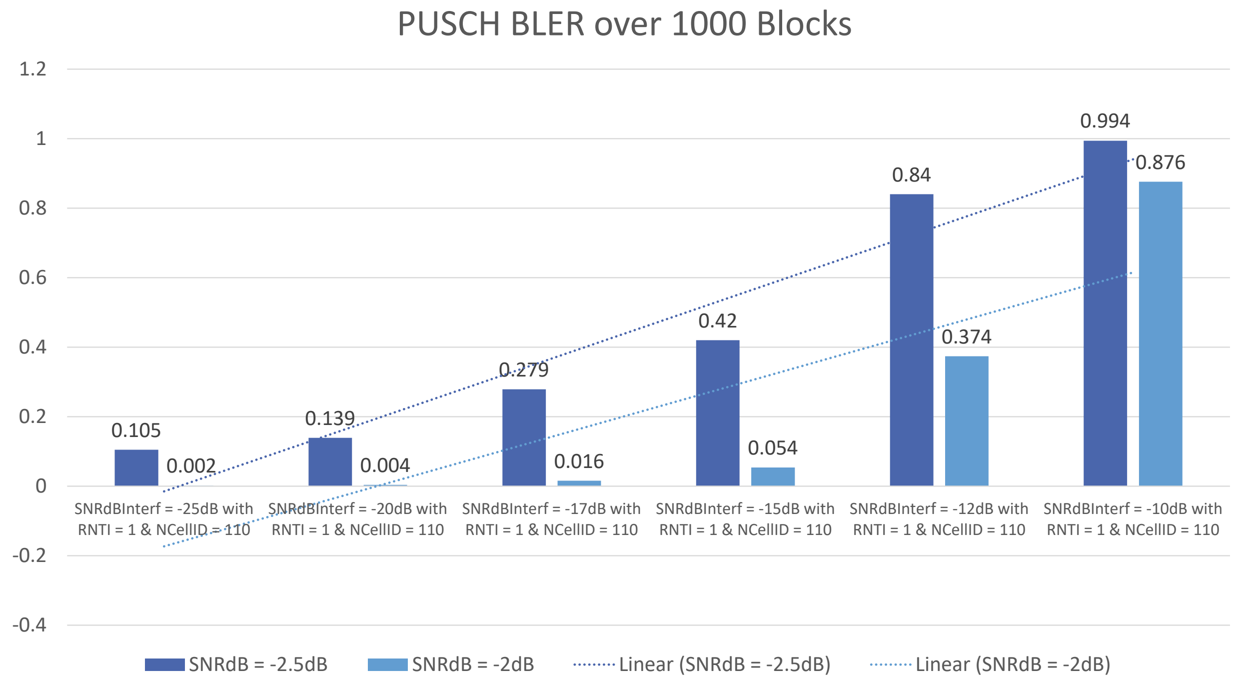

Figure 21. PUSCH BLER for NCellID = 110 with varying SNR and inter-cell interference levels

5.5. Discussion

The results from the performance evaluation of NR-PRACH and NR-PUSCH under both intra-cell and inter-cell interference conditions provide critical insights into the behavior and resilience of these key 5G components in realistic network environments.

The modeling approach used to simulate intra-cell interference by introducing an "Interfering" UE within the same cell as the "Target" UE successfully captures the expected real-world scenario where UEs share the same "Logical Sequence Index" but differ in "Preamble Index" values. This setup effectively replicates the interference dynamics that occur in densely populated cells where multiple UEs attempt to access the network simultaneously.

In the case of NR-PRACH, the simulation results (as shown in Figures 7 and 8) reveal that PRACH's performance, specifically the preamble detection probability, decreases significantly as the level of intra-cell interference increases. For instance, at an SNRdB of -10 dB for the Interfering UE, the preamble detection probability dropped by approximately 30% compared to low interference scenarios. This outcome aligns with theoretical expectations, as higher levels of interference typically degrade signal quality, making it more challenging for the receiver to correctly detect the preamble. Interestingly, the degradation in performance was observed regardless of the specific Preamble Index used by the Interfering UE, suggesting that the intra-cell interference exerts a uniform adverse effect on PRACH performance.

Furthermore, the results from varying the Preamble Index while maintaining a constant interference level (Figures 9 and 10) indicate that certain Preamble Index values offer better resilience to interference, particularly at moderate interference levels. For example, when the SNRdB was set to -23 dB, the preamble detection probability varied by up to 20% across different Preamble Index values, highlighting the potential for optimizing Preamble Index assignments to mitigate the effects of intra-cell interference, thereby improving the robustness of NR-PRACH in such conditions.

Similarly, the performance of NR-PRACH under inter-cell interference was modeled by placing the Interfering UE in a neighboring cell, using a different "Logical Sequence Index" but potentially sharing the same "Preamble Index" as the Target UE. The results (Figures 11 and 12) show a consistent degradation in PRACH performance as the level of inter-cell interference increases. For instance, the detection probability dropped by nearly 35% when the SNRdB of the Interfering UE increased from -25 dB to -10 dB. This behavior is in line with expectations, as signals from adjacent cells can overlap and cause significant interference, particularly in scenarios with high UE density.

When analyzing the influence of different RootSequenceIndex values on PRACH performance (Figures

13 and 14), the results indicate that some RootSequenceIndex values are more susceptible to interference than others, especially under high interference conditions. For example, at an SNRdB of -9 dB, the detection probability for a RootSequenceIndex of 1 was 25% lower than that for a RootSequenceIndex of 4. This finding suggests that careful selection of RootSequenceIndex values could be a viable strategy to enhance the resilience of PRACH in multi-cell environments.

For NR-PUSCH, the evaluation under intra-cell interference conditions (Figures 15 to 18) demonstrated a clear inverse correlation between SNR and Block Error Rate (BLER), where higher SNR levels significantly improve reception quality, reducing BLER. Specifically, at an SNR of -2.5 dB, the BLER was nearly 100%, but it dropped to less than 1% when the SNR improved to -1 dB. The results also showed that different RNTI values influence the sensitivity of NR-PUSCH to intra-cell interference, with BLER reductions ranging between 15% to 25% as SNR increased, indicating that certain configurations might offer better resistance to interference.

In the case of inter-cell interference (Figures 19 to 21), the results consistently showed that increased interference from neighboring cells leads to a higher BLER. For example, when the SNRdBInterf increased from -25 dB to -10 dB, the BLER escalated from around 11.5% to nearly 100%, demonstrating the vulnerability of NR-PUSCH to inter-cell interference. The findings also suggest that different NCellID configurations may impact the sensitivity of NR-PUSCH to inter-cell interference, with variations of up to 2% in BLER across different configurations under identical conditions.

Overall, the results underscore the importance of considering both intra-cell and inter-cell interference when designing and optimizing NR-PRACH and NR-PUSCH systems. The findings suggest that tailored interference management strategies, such as optimizing Preamble Index, RootSequenceIndex, and RNTI configurations, could significantly enhance the robustness and efficiency of 5G NR systems in environments characterized by high levels of interference.

6. Conclusion and Future Works

This study has provided an in-depth analysis of how intra-cell and inter-cell interference significantly affects NR-PUSCH performance in 5G networks. Through extensive simulations on MATLAB, we illustrated how factors such as user scheduling, power control, cell ID, and RNTI configuration can collectively influence uplink throughput by up to 30% in dense intra-cell scenarios and 25% in multi-cell deployments.

6.1. Key Insights and Contributions:

- Effective Interference Management: Our results confirm that optimizing scheduling and power control can mitigate the performance drop from simultaneous transmissions, leading to throughput gains of around 15%. In densely populated cells, advanced interference management techniques (interference cancellation, suppression) further enhance PUSCH reliability.
- UE Configuration and Cell Planning: The identification of specific UE configurations (e.g., RNTI assignment) and strategic cell planning (e.g., controlling overlapping frequencies) proved essential in reducing contention on PUSCH resources.
- Complexity vs. Real-Time Constraints: Although sophisticated interference mitigation strategies are beneficial, their computational overhead may limit applicability in real-time networks, stressing the need for scalable solutions.

6.2. Applications in Evolving 5G Environments:

- Massive MIMO Systems: The introduction of large-scale antenna arrays in 5G can amplify both the benefits and challenges of interference management. While beamforming and spatial multiplexing increase capacity, they also demand more refined scheduling and power control strategies to avoid inter- and intra-cell interference.
- Network Slicing: In 5G networks supporting multiple slices (eMBB, URLLC, mMTC), diverse latency and reliability requirements demand flexible interference management. Our findings on dynamic parameter tuning (e.g., RNTI assignment, root sequences) could be integrated into slice-aware resource orchestration, ensuring each slice meets its QoS targets.

6.3. AI, ML, and Emerging 6G Technologies:

Future networks are envisioned to be increasingly autonomous, leveraging machine learning and AI for proactive interference prediction and adaptive resource allocation. Deep learning frameworks could identify complex interference patterns, while reinforcement learning approaches might dynamically reconfigure scheduling and power levels in real time. Moreover, looking ahead to 6G, technologies such as Reconfigurable Intelligent Surfaces (RIS) and advanced THz communication paradigms will introduce new ways to manipulate radio propagation and further reduce interference. The strategies proposed hereÂŮoptimizing PUSCH configurations, cell IDs, and resource managementÂŮcould be extended and enhanced by these emerging techniques.

6.4. Limitations and Future Directions:

- Extended Scenarios: The simulations relied on controlled testbeds with limited bandwidth and specific power control settings. Real-world systems often exhibit larger bandwidths and diverse mobility profiles, so testing across varied environments (e.g., mmWave, high-speed vehicular) is crucial.
- Adaptive Interference Management: Building on our results, future work could incorporate AI-driven solutions that adapt interference mitigation strategies on-the-fly. For instance, advanced ML models might forecast interference bursts and proactively adjust scheduling, power, or preamble resources.
- Integration with ML and SON: Investigating how Self-Organizing Networks (SON) and orchestrators use distributed intelligence to coordinate cross-cell interference management (e.g., dynamic root sequence reallocation) will be valuable as densification accelerates.
- Joint Uplink-Downlink Optimization: While this study focused on PUSCH, a holistic approach to interference management requires balancing uplink and downlink demands. Future research may explore joint scheduling frameworks for more efficient resource usage.

In conclusion, efficiently managing interference remains pivotal to unlocking the full potential of 5G-NR networks. Our findings emphasize that strategic parameter tuning, coupled with advanced interference cancellation and suppression mechanisms, can yield substantial gains. With the integration of AI, ML, and next-generation 6G features like RIS, these strategies can evolve into adaptive, intelligent interference management solutions suitable for diverse 5G applicationsÂŮfrom massive MIMO deployments to slice-based service orchestration.

References

[1] E. Dahlman, S. Parkvall, and J. Skold. *5G NR: The next generation wireless access technology*. Academic Press, 2020.

[2] B. Bertenyi, S. Nagata, H. Kooropaty, X. Zhou, W. Chen, Y. Kim, X. Dai, and X. Xu. “5G NR radio interface”. In: *Journal of ICT Standardization* 6.1-2 (2018), pages 31–58. DOI: 10.13052/jicts2245-800x.613.

[3] S. Parkvall, Y. W. Blankenship, R. Blasco, E. Dahlman, G. Fodor, S. J. Grant, E. Stare, and M. Stattin. “5G NR Release 16: Start of the 5G Evolution”. In: *IEEE Commun. Stand. Mag.* 4.4 (2020), pages 56–63. DOI: 10.1109/MCOMSTD.011.1900018. URL: https://ieeexplore.ieee.org/document/9316432.

[4] S. Ahmadi. *5G Network Architecture*. 2019. DOI: 10.1016/b978-0-08-102267-2.00001-4. URL: https://linkinghub.elsevier.com/retrieve/pii/B9780081022672000014.

[5] A. Mukherjee. *5G New Radio: Beyond Mobile Broadband*. Artech House, 2019. ISBN: 9781630816421. URL: https://www.artechhouse.com/Products/5G-New-Radio-Beyond-Mobile-Broadband-3758.aspx.

[6] B. Ozpoyraz, A. T. Dogukan, Y. Gevez, U. Altun, and E. BaÅ§ar. “Deep Learning-Aided 6G Wireless Networks: A Comprehensive Survey of Revolutionary PHY Architectures”. In: *IEEE Open Journal of the Communications Society* 3 (2022), pages 1749–1809. DOI: 10.1109/ojcoms.2022.3210648. URL: https://ieeexplore.ieee.org/document/9905727.

[7] E. C. V. Boas, J. D. S. e Silva, F. A. D. de Figueiredo, L. Mendes, and R. D. de Souza. “Artificial intelligence for channel estimation in multicarrier systems for B5G/6G communications: a survey”. In: *EURASIP Journal on Wireless Communications and Networking* 2022 (2022), pages 1–63. DOI: 10.1186/s13638-022-02195-3. URL: https://doi.org/10.1186/s13638-022-02195-3.

[8] M. Shammaa, M. Mashaly, and A. El-Mahdy. “A deep learning-based adaptive receiver for full-duplex systems”. In: *AEU - International Journal of Electronics and Communications* null (2023), null. DOI: 10.1016/j.aeue.2023.154822. URL: https://www.sciencedirect.com/science/article/abs/pii/S1434841123002960?via=ihub.

[9] A. S. Doshi, M. Gupta, and J. Andrews. “Over-the-Air Design of GAN Training for mmWave MIMO Channel Estimation”. In: *IEEE Journal on Selected Areas in Information Theory* 3 (2022), pages 557–573. DOI: 10.1109/jsait.2022.3222479. URL: https://ieeexplore.ieee.org/document/9953094.

[10] H. dos Santos Sousa, J. A. Soares, K. S. Mayer, and D. Arantes. “CVNN-based Channel Estimation and Equalization in OFDM Systems Without Cyclic Prefix”. In: *ArXiv* abs/2308.13623 (2023), null. DOI: 10.14209/sbrt.2023.1570923809. URL: https://arxiv.org/abs/2308.13623.

[11] S.-W. Jeon and C. Suh. “Degrees of freedom of uplink-downlink multiantenna cellular networks”. In: *2014 IEEE International Symposium on Information Theory* null (2014), pages 1593–1597. DOI: 10.1109/isit.2014.6875102. URL: https://ieeexplore.ieee.org/document/6875102.

[12] A. B. Dayi. “Improving 5g nr uplink channel estimation with artificial neural networks: a practical study on NR PUSCH receiver”. In: *2022 IEEE International Black Sea Conference on Communications and Networking (BlackSeaCom)*. IEEE. 2022, pages 129–134. DOI: 10.1109/blackseacom54372.2022.9858290. URL: https://ieeexplore.ieee.org/document/9858290.

[13] R. Fang, H. Chen, and W. Liu. “Deep Learning-Based PRACH Detection Algorithm Design and Simulation”. In: *2022 2nd International Conference on Frontiers of Electronics, Information and Computation Technologies (ICFEICT)*. 2022, pages 505–511. DOI: 10.1109/ICFEICT57213.2022.00094. URL: https://ieeexplore.ieee.org/document/10009473.

[14] G. Schreiber and M. Tavares. “5G New Radio Physical Random Access Preamble Design”. In: *2018 IEEE 5G World Forum (5GWF)*. 2018, pages 215–220. DOI: 10.1109/5GWF.2018.8517052. URL: https://ieeexplore.ieee.org/document/8517052.

[15] Q. Xiong, B. Yu, C. Qian, X. Li, and C. Sun. “Random Access Preamble Generation and Procedure Design for 5G-NR System”. In: *2018 IEEE Globecom Workshops (GC Wkshps)*. 2018, pages 1–5. DOI: 10.1109/glocomw.2018.8644175. URL: https://ieeexplore.ieee.org/document/8644175.

[16] P. Gu, Y. Song, and C. Liu. “Channel Estimation of mmWave Massive MIMO System Based on Manifold Learning”. In: *2022 IEEE 22nd International Conference on Communication Technology (ICCT)* null (2022), pages 1004–1008. DOI: 10.1109/icct56141.2022.10073197. URL: https://ieeexplore.ieee.org/document/10073197.

[17] Y. Li, X. Bian, and M. Li. “Denoising Generalization Performance of Channel Estimation in Multipath Time-Varying OFDM Systems”. In: *Sensors (Basel, Switzerland)* 23 (2023), null. DOI: 10.3390/s23063102. URL: https://www.mdpi.com/1424-8220/23/6/3102.

[18] Y. Sun, Y. Cheng, T. Liu, Q. Huang, J. Guo, and W. Jin. “Research on Signal Detection of OFDM Systems Based on the LSTM Network Optimized by the Improved Chameleon Swarm Algorithm”. In: *Mathematics* null (2023), null. DOI: 10.3390/math11091989. URL: https://www.mdpi.com/2227-7390/11/9/1989.

[19] S. Haq, A. K. Gizzini, S. Shrey, S. Darak, S. Saurabh, and M. Chafii. “Deep Neural Network Augmented Wireless Channel Estimation for Preamble-Based OFDM PHY on Zynq System on Chip”. In: *IEEE Transactions on Very Large Scale Integration (VLSI) Systems* 31 (2022), pages 1026–1038. DOI: 10.36227/techrxiv.20443917. URL: https://ieeexplore.ieee.org/document/10129990.

[20] C. Song, X. Zhou, C. Wang, and Z. Ye. “A Double-Threshold Channel Estimation Method Based on Adaptive Frame Statistics”. In: *Mathematics* null (2023), null. DOI: 10.20944/preprints202306.1247.v1. URL: https://www.mdpi.com/2227-7390/11/15/3342.

[21] I. Shomorony and A. Avestimehr. “Multihop Wireless Networks: A Unified Approach to Relaying and Interference Management”. In: *Found. Trends Netw.* 8 (2014), pages 149–280. DOI: 10.1561/1300000044. URL: https://www.nowpublishers.com/article/Details/NET-044.

[22] Huawei. *R1-071409: Efficient Matched Filters for Paired Root Zadoff-Chu Sequences*. 3GPP TSG RAN WG1, meeting 48bis, St Julians, Malta. Available online at https://www.3gpp.org/ftp/tsg_ran/WG1_RL1/TSGR1_48bis/Docs/R1-071409.zip. 2007.

[23] S. Sesia, I. Toufik, and M. Baker. *LTE âĂŞ The UMTS Long Term Evolution: From Theory to Practice*. John Wiley & Sons, 2011. ISBN: 9780470660256. DOI: 10.1002/9780470978504. URL: https://onlinelibrary.wiley.com/doi/book/10.1002/9780470978504.

[24] Z. Shawqi and S. Y. Ameen. “Deep Learning Based Channel Estimation for 5G and Beyond”. In: *IEEE Communications Surveys & Tutorials* (2023). DOI: 10.26682/csjuod.2023.26.2.46.

[25] W. Du, Z. Liu, and F. Li. “Interference Neutralization With Partial CSIT for Full-Duplex Cellular Networks”. In: *IEEE Access* 7 (2019), pages 49177–49190. DOI: 10.1109/access.2019.2910601. URL: https://ieeexplore.ieee.org/document/8688408/.

[26] P. Aquilina. “Advanced interference management techniques for future generation cellular networks”. In: (2017). URL: https://www.semanticscholar.org/paper/b20d3b0714e247f243a8d884108ebdc8b7a7cf54.

[27] M. Yang, S.-W. Jeon, and D. K. Kim. “On the Degrees of Freedom of Full-Duplex Cellular Networks”. In: *ArXiv* abs/1604.07957 (2016), null. URL: https://www.semanticscholar.org/paper/6a318964ad3ec6be0ec629205d0822cbf1b3989d.

[28] G. Sridharan. “Interference Alignment in Cellular Networks”. Available online at TSpace, University of Toronto. PhD thesis. University of Toronto, 2015. URL: https://utoronto.scholaris.ca/bitstreams/download.

[29] S. H. Chae and K. Lee. “Degrees of Freedom of Full-Duplex Cellular Networks: Effect of Self-Interference”. In: *IEEE Transactions on Communications* 65 (2017), pages 4507–4518. DOI: 10.1109/tcomm.2017.2719022. URL: https://ieeexplore.ieee.org/document/7956187.

[30] S.-W. Jeon, S. H. Chae, and S. Lim. “Degrees of freedom of full-duplex multiantenna cellular networks”. In: *2015 IEEE International Symposium on Information Theory (ISIT)* null (2015), pages 869–873. DOI: 10.1109/isit.2015.7282579. URL: https://ieeexplore.ieee.org/document/7282579.

[31] S.-W. Jeon and W.-Y. Shin. “Dynamic Opportunistic Interference Alignment for Random-Access Small-Cell Networks”. In: *The Journal of Korean Institute of Communications and Information Sciences* (2014), pages 675–681. DOI: 10.7840/KICS.2014.39A.11.675. URL: https://doi.org/10.7840/KICS.2014.39A.11.675.

[32] F. Launay. *Les rÃľseaux de mobiles 4G et 5G: PRACH*. Blog post. Accessed: August 12, 2024. 2022. URL: https://blogs.univ-poitiers.fr/f-launay/tag/prach/.

[33] Z. Guo, Y. Yuan, and Y. Chen. “5G NR Uplink Coverage Enhancement Based on DMRS Bundling and Multi-slot Transmission”. In: *2020 IEEE 20th International Conference on Communication Technology (ICCT)*. 2020, pages 482–486. DOI: 10.1109/ICCT50939.2020.9295747. URL: https://ieeexplore.ieee.org/document/9295747/.

[34] S. S. Demirsoy and K. Marks. “SoC framework for FPGA: A case study of LTE PUSCH receiver”. In: *2009 IEEE International SOC Conference (SOCC)*. IEEE. 2009, pages 29–32. DOI: 10.1109/soccon.2009.5398103. URL: https://ieeexplore.ieee.org/document/5398103.

[35] D. H. Morais. *5G NR Overview*. 2023. DOI: 10.1007/978-3-031-33812-0_8. URL: https://doi.org/10.1007/978-3-031-33812-0_8.

[36] S. Kannan and P. Viswanath. “Capacity of Multiple Unicast in Wireless Networks: A Polymatroidal Approach”. In: *IEEE Transactions on Information Theory* 60 (2011), pages 6303–6328. DOI: 10.1109/tit.2014.2347277. URL: https://ieeexplore.ieee.org/document/6877730/.

[37] The MathWorks, Inc. *MATLAB version: 9.13.0 (R2022b)*. Accessed: January 01, 2023. 2022. URL: https://www.mathworks.com.